

Time-Dependent Structure of the Upper Atmosphere

ISADORE HARRIS AND WOLFGANG PRIESTER¹

NASA Goddard Space Flight Center, Greenbelt, Md., and Institute for Space Studies, New York 27, N. Y.

(Manuscript received 20 April 1962)

ABSTRACT

The physical properties of the upper atmosphere are determined mainly by heat conduction, the heat sources and the barometric law. An analysis of the integro-differential equation which describes these physical processes has been carried out. It is found that heating of the thermosphere due to absorption of the solar extreme ultraviolet (EUV) radiation alone cannot explain the observed diurnal variation of density and temperature, since it would yield a maximum of these properties at about 17^h local time, instead of 14^h where it is observed. Secondly, if the EUV flux is adjusted to give the observed average temperature, then the diurnal variation in density would be much too large compared with the observed amplitude. Thirdly, it would require an extremely high efficiency for the conversion of EUV radiation into heat, if we compare the required flux with Hinteregger's measurements of the EUV flux. Thus, it is necessary to have another heat source in addition to the heating due to absorption of EUV radiation. If an additional heat source is used, which has a maximum at about 9^h local time and a flux of $1 \text{ erg cm}^{-2} \text{ sec}^{-1}$, a time-dependent model of the upper atmosphere is obtained that is in good agreement with the observed densities. There is evidence that this additional heat source derives its energy ultimately from the solar corpuscular radiation.

In this paper we present the results of calculations for a model in the equatorial and temperate zones of the earth, for those times when the average solar activity corresponds to a solar radiation flux of $200 \times 10^{-22} \text{ Wm}^{-2} (\text{cps})^{-1}$ at 10.7-cm wavelength. The physical properties (temperature, density, pressure, scale height, mean molecular weight and the number densities of N₂, O₂, O, He and H) are given as a function of local time and for the altitudes between 120 km and 2050 km.

I. Introduction

The energy balance of the upper atmosphere is determined mainly by absorption of solar energy and the heat transfer by conduction. These processes are described by the time-dependent equation for heat conduction and by the heat source functions. If these equations are combined with the equation for hydrostatic balance they yield the physical properties of the upper atmosphere as a function of time and altitude.

We have studied the solutions of these equations in detail by a process of numerical integration, and compared the results with time-dependent models derived from satellite density data, in order to obtain some information as to the nature of the heat sources of the upper atmosphere.

During the last three years, four main effects have been found to affect the physical properties of the upper atmosphere. This information was obtained mostly from analysis of the fluctuations in the orbital periods of artificial satellites. Any theoretical model of the upper atmosphere should be able to account for these phenomena. They are:

- (a) the solar activity effect,
- (b) the diurnal variation,
- (c) the geomagnetic activity effect, and
- (d) the semiannual variation.

(a) The solar activity effect is defined as the correlation found between density fluctuations in the altitude range from 200 km to 1600 km and the solar flux in the decimeter wavelength range (3 to 30 cm) (W. Priester, 1959; L. G. Jacchia, 1959 a, b; H. K. Paetzold, 1959; W. Priester and H. A. Martin, 1960; M. Roemer, 1961 a, b; P. E. Zadunaisky, I. I. Shapiro and H. M. Jones, 1961; R. Bryant, 1961). This correlation has again brilliantly been confirmed by L. G. Jacchia and J. Slowey (1962) in their analysis of the orbit of the twelve-foot balloon satellite (1961 delta 1).

The solar decimeter radiation cannot be the physical cause of the fluctuations but is merely an index of it. This radiation in the 3- to 30-cm wavelength range is the so-called "slowly varying component" which is produced, according to M. Waldmeier and H. Mueller (1950), by thermal emission from condensations in the solar corona. This flux is proportional to $A \int n_e n_i ds$, integrated along the ray path through the condensation. The symbols n_e and n_i represent the number densities of electrons and ions respectively and A is the projected area of the condensation.

It is believed that the solar activity effect in the

¹ National Academy of Sciences-National Research Council Senior Research Associate with the National Aeronautics and Space Administration; on leave from Bonn University Observatory.

upper atmosphere is caused to a large extent by the heating due to absorption (photoionization) of solar extreme ultraviolet (EUV) radiation. H. E. Hinteregger (1961) has shown from rocket observations that the absorption of this radiation takes place in the altitude range between 150 and 300 km.

The main process producing the emission lines in the extreme ultraviolet is likely to be the emission due to cascades following recombination on excited levels. Therefore, the total intensities of these lines can be expected also to be proportional to the above mentioned integral, if self-absorption is negligible. It is therefore reasonable to expect a close correlation between the decimeter flux and the strongest lines in the extreme ultraviolet range of the solar spectrum (He II 304 Å, He I 584 Å and numerous lines of highly ionized atoms), since these lines should also originate mostly in the coronal condensations.

The factor of proportionality between density and the decimeter flux is observed to be a function of height and also local time—being larger during the nighttime. This behavior is to be expected from the diurnal variation of the temperature in the atmosphere (W. Priester, 1961; L. G. Jacchia, 1961).

(b) The diurnal density variation has an amplitude which increases with altitude. At 210 km it is only a few per cent of the mean value. This result was obtained from the orbital analysis of 1958 delta 1 and 2 (Sputnik III rocket and satellite) by W. Priester, H. A. Martin and K. Kramp (1960). At an altitude of 650 km, however, the amplitude reaches a factor of almost ten, as found by W. Priester and H. A. Martin (1960), L. H. Jacchia (1960), H. K. Paetzold and H. Zschoerner (1960), D. G. King-Hele and D. M. C. Walker (1960). The data showing this effect were obtained mostly from satellites 1958 beta 2 (Vanguard I) and 1959 alpha 1 (Vanguard II). These data also revealed that the diurnal variation in density reaches its peak density at approximately 14^h local time followed by a decline; then at about sunrise the density begins to increase rapidly to its peak value again. This behavior results from the combined action of a time-dependent heat source and thermal conduction. This was clearly pointed out by M. Nicolet (1960).

(c) The geomagnetic activity effect in the upper air densities was noted by L. G. Jacchia (1959) as a correlation between short-lived density fluctuations and the geomagnetic activity represented by the K_p or A_p indices. It was confirmed by density data obtained from seven satellites during the so-called "November 1960 events" (L. G. Jacchia, 1961a; G. V. Groves, 1961). It was also confirmed by R. Jastrow and R. Bryant (1961), who used the data from Echo I, and was further verified by H. K. Paetzold (1960) using the data from Sputnik II (1958 delta 2). The closest correlation of this kind has been obtained with data

from the 12-ft balloon satellite (1961 delta 1) by L. G. Jacchia and J. Slowey (1961).

This effect strongly suggests the existence of another heat source in addition to the absorption of solar EUV-radiation. It seems plausible to attribute this additional heat source to energy that is ultimately derived from the solar corpuscular radiation or its "steady" component, the solar wind.

(d) The existence of such an additional heat source also is suggested by the fourth effect, a semiannual variation in atmospheric density found by H. K. Paetzold and H. Zschoerner (1960). They observed variations in which the densities have maxima in March and September and minima in June and July and also in December and January. This behavior is quite similar to the semiannual variation of geomagnetic activity, found by A. L. Cortie (1912) and discussed in great detail by J. Bartels (1932).

H. K. Paetzold and H. Zschoerner (1961) estimate that a decrease of 0.2 erg cm⁻² sec⁻¹ in the over-all flux used for heating during the periods of minima (June-July and December-January) is required to explain the observed decrease in density. This suggests that the second heat source, which we shall call a "corpuscular" heat source, normally provides an energy flux which is a few times larger than the above mentioned value of 0.2 erg cm⁻² sec⁻¹. A crude estimate may also be obtained from the absolute value of and the variation of the geomagnetic u -measure which was defined by J. Bartels (1932) as the "inter-diurnal variability of the horizontal component at the geomagnetic equator." In a recent paper by W. Priester and D. Cattani (1962) the semiannual variation of the u -measure was related to a model of the solar corpuscular radiation dependent on heliographic latitude.

In view of this relationship and with roughly 20 per cent semiannual variation in the amplitude of the u -measure, we might expect a total flux in the order of 1 erg cm⁻² sec⁻¹ for the "corpuscular" heat source. As the measurements from Explorer X by H. S. Bridge *et al.* (1961) revealed a flux of about 5 erg cm⁻² sec⁻¹ for the solar wind outside the earth's magnetosphere, our estimate of 1 erg cm⁻² sec⁻¹ for the "corpuscular" heat source seems to be plausible. Since this heat source is likely to have a diurnal variation, the estimated flux given refers to the diurnal peak value.

These conclusions are supported by the results obtained from our calculations of the energy balance of the upper atmosphere in which the time-dependent heat conduction equation was used with the condition of quasi-hydrostatic equilibrium. These results showed that a theoretical explanation of the observed atmospheric densities can only be obtained by taking into account a second heat source, which contributes roughly the same amount of heat to the upper atmosphere as the EUV heat source.

In our solution which represents the observed

densities, we used a peak flux of $0.93 \text{ erg cm}^{-2} \text{ sec}^{-1}$ for the fraction of the solar EUV radiation which is converted into heat and a peak flux of $1.03 \text{ erg cm}^{-2} \text{ sec}^{-1}$ for the "corpuscular" heat source.

2. The heat conduction equation for a gas in equilibrium with a gravitational field

The temperature distribution of the upper atmosphere is mainly governed by thermal conduction and absorption of solar energy (see L. Spitzer, 1949; and M. Nicolet, 1961a). As the temperature undergoes a diurnal variation, the upper atmosphere expands and contracts. This expansion and contraction produces a transfer of heat by mass flow. In the motion of the thermosphere, energy is expended or gained because of the work done against or by gravity. In this section we shall give an heuristic derivation of the appropriate equation, which will contain an expansion-contraction term allowing for the heat transfer due to the diurnal "breathing" of the thermosphere and the work done by or against gravity.

We use Eq (9-6) of C. Eckart (1960) for the temperature dependence of a gas undergoing a flow in an external gravity field. We simplify to one dimension and express it in our own notation.

$$\frac{\partial T_1}{\partial t} + \frac{\partial T_0}{\partial z} w + \frac{\gamma-1}{a_0} \frac{\partial w}{\partial z} = \frac{q}{C_v}. \quad (1)$$

The above is one of the linearized equations of hydrodynamics in which:

T_1 =the perturbed temperature,

w =the vertical velocity of the gas,

T_0 =the initial temperature distribution at any initial time,

C_v =the heat capacity at constant volume,

γ =the ratio of the specific heats,

a_0 =the coefficient of thermal expansion, which is $1/T_0$ for an ideal gas, and

q =the net gain of heat (in erg/g·sec) due to heat sources and conduction.

We shall give the detailed expression for q later.

The derivation will be given for a gas with a single constituent, but we shall generalize later to a multi-constituent thermosphere.

We shall obtain a form for w which is based upon considerations used by ionospheric physicists in the study of the drift motions of the F2 max level of the ionosphere (see J. A. Ratcliffe and K. Weeks, 1960). As the atmosphere expands and contracts, we shall assume that a cell of gas reaches an altitude $z+w\Delta t$, at a time $t+\Delta t$, where the pressure is the same as at the altitude z at the previous time t . That means

$$p(z+w\Delta t, t+\Delta t) = p(z, t).$$

Since this motion is very slow (in the order of 10 km hr⁻¹ at 500 km), we shall also assume that the pressure to first order follows the barometric law.

Thus we have

$$p_0 \exp \left[- \int_0^{z+w\Delta t} gM/RT(t+\Delta t) dz' \right] \\ = p_0 \exp \left[- \int_0^z gM/RT(t) dz' \right],$$

where g is the acceleration due to gravity, R the universal gas constant and p_0 can be taken as the pressure at the earth's surface, which for our purposes is constant. We expand the above in powers of Δt according to

$$\frac{1}{T(t+\Delta t)} = \frac{1}{T(t)} \left(1 - \frac{1}{T(t)} \frac{\partial T}{\partial t} \Delta t \right)$$

and obtain

$$w = T \int_0^z \frac{1}{T^2} \frac{\partial T}{\partial t} dz'. \quad (2)$$

In the spirit of the linearized Eq (1) we should write

$$w = T_0 \int_0^z \frac{1}{T_0^2} \frac{\partial T}{\partial t} dz'. \quad (2')$$

We thus have also

$$\frac{\partial w}{\partial z} = \frac{\partial T_0}{\partial z} \int_0^z \frac{1}{T_0^2} \frac{\partial T}{\partial t} dz' - \frac{1}{T_0} \frac{\partial T}{\partial t}.$$

Substituting into Eq (1) we obtain

$$\frac{\partial T_1}{\partial t} + \frac{\partial T_0}{\partial z} T_0 \int_0^z \frac{1}{T_0^2} \frac{\partial T_1}{\partial t} dz' + (\gamma-1) \frac{\partial T_1}{\partial t} = \frac{q}{C_v}$$

or

$$\frac{\partial T_1}{\partial t} + \frac{\partial T_0}{\partial z} T_0 \int_0^z \frac{1}{T_0^2} \frac{\partial T_1}{\partial t} dz' = \frac{q}{C_p}, \quad (3)$$

where C_p is the specific heat at constant pressure.

Eq (3) is our basic equation. We shall integrate it numerically where for T_0 , $\partial T_0/\partial z$ and the non-linear terms that appear in q , we shall take their values at $t-\Delta t$, where Δt is our integration interval. In this fashion we determine new initial solutions to be used as the unperturbed functions T_0 in each step of the integration process. Thus our numerically determined perturbed solutions shall not differ greatly from our unperturbed solutions at any time. With this understanding for the treatment of the non-linear terms, we drop the subscripts 1 and 0.

The 2nd term on the left hand side of Eq (3), being

proportional to the gradient of the temperature, represents a mode of "convective" transport of heat due to the diurnal expansion and contraction—a free expansion of a nonisothermal gas in a gravitational field—as mentioned earlier. In its present form it also includes partially the effects of gravity. The main effect of gravity in the heat balance is contained in the right hand side of Eq (3) where instead of C_v , C_p appears.

It remains to be shown that our assumptions leading to the expression for w are consistent with Eckart's Eq (9-5) for the variation of the perturbed pressure, which in our notation (one dimension) is

$$\frac{\partial p_1}{\partial t} + \frac{\partial p_0}{\partial z} w + \rho_0 \gamma \frac{RT_0}{M} \frac{\partial w}{\partial z} = (\gamma - 1) \rho_0 q \quad (4)$$

where p_0 is the unperturbed pressure and ρ_0 the unperturbed density.

From hydrostatic equilibrium, we have $d\rho_0/dz = -\rho_0 g$ and substituting in the expression for w we obtain

$$\frac{\partial p_1}{\partial t} = \rho_0 g T \int_0^z \frac{1}{T_0^2} \frac{\partial T}{\partial z'} dz',$$

or from the perfect gas law $p = \rho RT/M$ we have

$$\frac{\partial \rho_1}{\partial t} = -\frac{\rho_0}{T} \frac{\partial T_1}{\partial t} + \frac{g \rho_0 M}{R} \int_0^z \frac{1}{T^2} \frac{\partial T}{\partial z'} dz'. \quad (5)$$

From the conservation of mass we have

$$\frac{\partial}{\partial t} \int_0^\infty \rho dz = \int_0^\infty \frac{\partial \rho}{\partial t} dz = 0. \quad (6)$$

Thus we obtain by integrating Eq (5) over z

$$\int_0^\infty \frac{\rho_0}{T} \frac{\partial T}{\partial t} dz = \int_0^\infty dz \frac{g \rho_0 M}{R} \int_0^z dz' \frac{1}{T(z')^2} \frac{\partial T(z')}{\partial t}. \quad (6a)$$

The double integral on the right hand side of this equation can be transformed in the following manner. It is an integral over an area in the (z, z') plane bounded by the z -axis and the $z=z'$ line. The order of the integration can be changed by first integrating with respect to z from $z=z'$ to $z=\infty$, and then over z' from 0 to $z'=\infty$. Thus the equation becomes

$$\int_0^\infty \frac{\rho_0}{T} \frac{\partial T_1}{\partial t} dz = \int_0^\infty \frac{1}{T_0(z')^2} \frac{\partial T(z')}{\partial t} \left[\int_{z'}^\infty \frac{g M}{R} \rho_0(z) dz \right] dz'.$$

If the above is to be true for all possible variations of $\partial T/\partial t$ we must have

$$\rho_0 = \frac{1}{T_0} \int_z^\infty \frac{g M}{R} \rho_0(z') dz',$$

which is another form of the barometric law in the case of a non-isothermal atmosphere. This can be seen by differentiating the above with respect to z to obtain

$$\frac{\partial \rho_0}{\partial z} = -\frac{1}{T} \frac{g M}{R} \rho_0 - \frac{1}{T_0^2} \frac{\partial T_0}{\partial z} \int_z^\infty \frac{g M}{R} \rho(z') dz'$$

and using (6a) again we have

$$\frac{\partial \rho_0}{\partial z} = -\frac{1}{T_0} \frac{g M}{R} \rho_0 - \frac{\rho_0}{T_0} \frac{\partial T_0}{\partial z},$$

or, integrating we have

$$\frac{\rho_0}{\rho_{00}} = \frac{T_{00}}{T_0} \exp \left[- \int_0^z \frac{g M}{R T_0} dz' \right] \quad (7)$$

where ρ_{00} , T_{00} are the values of ρ_0 , T_0 , respectively, at $z=0$.

Thus, we see that the assumption of hydrostatic equilibrium (in the approximation of the linearized equations) for deriving w is consistent with the equation for the variation of pressure with time. We can integrate the time dependent Eq (3), assuming that (7) holds at any instant of time.

We shall generalize the above for a multi-constituent thermosphere.

We now give the expression for q . We write

$$q\rho = Q_{\text{cond}} + Q_{\text{euv}} + Q_{\text{ox}} + Q'.$$

The term Q_{cond} is the net gain of heat by conduction. It is given by

$$Q_{\text{cond}} = \frac{\partial}{\partial z} \left(K(T) \frac{\partial T}{\partial z} \right) \quad (8)$$

where $K(T)$ is the coefficient of heat conduction and is taken to be

$$K(T) = \frac{\sum_i A_i n_i(z)}{\sum_i n_i(z)} T^{\frac{1}{2}}(z). \quad (9)$$

A_i is a constant depending upon the constituent i , and n_i is the number density of atoms or molecules of the i^{th} constituent.

We have from S. Chapman and T. G. Cowling (1960) (see also M. Nicolet, 1961b) the following values in erg $\text{cm}^{-1} \text{sec}^{-1} (\text{deg } K)^{-\frac{1}{2}}$:

$$A(\text{H}) = 2.1 \times 10^3,$$

$$A(\text{He}) = 9.0 \times 10^2,$$

$$A(\text{O}) = 3.6 \times 10^2, \text{ and}$$

$$A(\text{O}_2, \text{N}_2) = 1.8 \times 10^2.$$

The heat source due to the absorption of the solar EUV-radiation is given by

$$Q_{\text{euv}} = \sum_i \epsilon_i n_i(z) \int_0^\infty d\lambda F_\lambda \sigma_i(\lambda) e^{-\tau_i(\lambda, z, t)} \quad (10)$$

where

$$\tau_i(\lambda, z, t) = \int_z^\infty \sigma_i(\lambda) \frac{n_i(z')}{\cos \theta} dz.$$

$\sigma_i(\lambda)$ is the cross-section for absorption by the i^{th} constituent of radiation of wavelength λ in the region $d\lambda$, F_λ is the incident flux of wavelength λ in the region $d\lambda$ at the top of the atmosphere and ϵ_i is an efficiency factor for the conversion to thermospheric heat of energy in the extreme ultraviolet absorbed by the i^{th} constituent. θ is the zenith angle of the sun.

Q_{ox} is the heat loss due to the cooling by atomic oxygen radiating in the infrared and is given according to D. R. Bates (1951) by

$$Q_{\text{ox}} = -n_0 f(T),$$

$$f(T) = E_1 A_{12} \left[\frac{W_1 \exp\left(-\frac{E_1}{kT}\right)}{W_2 + W_1 \exp\left(-\frac{E_1}{kT}\right) + W_0 \exp\left(-\frac{E_0}{kT}\right)} \right]$$

where n_0 is the number density of atomic oxygen, E_1 the difference in energy between the $3P_1$ and $3P_2$ levels of atomic oxygen, E_0 the difference in energy between the $3P_0$ and $3P_2$ levels of atomic oxygen and W the statistical weights of the various levels and A_{12} the Einstein coefficient for the transition $3P_1 - 3P_2$.

The observations of the geomagnetic activity effect and of the semiannual effect strongly indicate the existence of another heat source, the energy of which is very likely provided finally by the solar corpuscular radiation and/or its steady component, the solar wind, for which we reserve a quantity Q' in our basic formula. Detailed considerations about this source are given later.

We need the expression for the total heat capacity at constant pressure, which we take as

$$\rho C_p = \sum_i n_i(z) k B_i;$$

where k is the Boltzmann constant and B_i is a constant depending upon the constituent. We have

$$B_i = 3.5 \text{ for diatomic molecules}$$

$$B_i = 2.5 \text{ for monatomic molecules.}$$

We rewrite Eq. (3) as

which we shall integrate numerically, linearizing by evaluating the non-linear factors from the values of the temperatures and densities at the previous time step in the integration procedure. All quantities in Eq (11) depend on altitude z and time t . Once the temperature profile is determined, the number densities n_i are calculated by means of the barometric relationship

$$n_i(z, t) = n_i(z_0) \frac{T(z_0)}{T(z, t)} \exp \left[- \int_{z_0}^z \frac{m_i g(z')}{k T(z', t)} dz' \right]. \quad (12)$$

The numerical procedure used to integrate Eq (11) was the implicit method (see G. B. Diaz *et al.*, 1958) for solving parabolic equations. This avoids the problem of instability which can arise from application of the explicit method (see A. N. Lowan, 1955).

The boundary conditions are a given initial temperature distribution, the temperature and densities of the constituents at the lower boundary held constant in time, and a zero gradient of the temperature at the upper boundary. The numerical integration was performed on an IBM 7090 computer.

Various integration intervals in time and space were tested and $\Delta t = 0.25$ hr and $\Delta z = 1$ km were found to be satisfactory. The temperature gradient was set equal to zero at the upper boundary, which we took to be 1000 km. An upper boundary at this altitude assures that the gradient in the temperature goes smoothly to zero.

Various initial temperature profiles were tried to test how rapidly the results converge to a final steady temperature profile of diurnal variation. It was found that this procedure necessitated integrating over a time corresponding to four or five days in real time in order to achieve this convergence, regardless of the initial temperature profile.

A small quantity equal to 10^{-3} was added to $\cos \theta$ to avoid the divergence when $\cos \theta$ goes to zero. This corresponds to an error of $\frac{2}{3}$ of a minute in time.

During the computations it was found that the "convective" term corresponding to heat transport caused by the diurnal variation of the temperature is small. It decreases the mean diurnal temperature of the exosphere by less than 5 per cent.

The total pressure was computed by summing up the partial pressures due to each constituent, which was calculated from the perfect gas law

$$p_i(z, t) = n_i(z, t) k T(z, t). \quad (13)$$

$$\boxed{\frac{\partial}{\partial z} \left(K(T) \frac{\partial T}{\partial z} \right) - \rho C_p \frac{\partial T}{\partial z} T \int_0^z \frac{1}{T^2} \frac{\partial T}{\partial z} dz' + Q_{\text{euv}} + Q_{\text{ox}} + Q' = \rho C_p \frac{\partial T}{\partial t}} \quad (11)$$

The total density was calculated by means of

$$\rho(z,t) = \sum_i n_i(z,t) m_i \quad (14)$$

where m_i is the mass in grams of the i^{th} type of molecule. Then the mean molecular weight was calculated from

$$M(z,t) = \frac{\sum_i n_i(z,t) M_i}{\sum_i n_i(z,t)}. \quad (15)$$

Finally the scale height was computed by means of

$$H(z,t) = \frac{RT(z,t)}{M(z,t)g(z)}. \quad (16)$$

The densities at heights greater than 1000 km were computed by the following method. In the isothermal region we have

$$n_i(z,t) = n_i(z_m,t) \exp \left[-\frac{m_i}{kT_m(t)} \int_{z_m}^z g(z') dz' \right] \quad (17)$$

where T_m is the temperature in the isothermal region which begins at the altitude z_m , which we took equal to the upper boundary of our integration ($z_m = 1000$ km).

We have for the acceleration of gravity:

$$g(z) = g_m \left(\frac{R_m}{R_m - z_m + z} \right)^2 \quad (18)$$

where g_m is the acceleration of gravity at the distance R_m from the center of the earth, at height z_m .

Integrating we have

$$n_i(z,t) = n_i(z_m,t) \exp \left[-\frac{m_i g_m R_m}{kT_m(t)} \frac{z - z_m}{R_m - z_m + z} \right] \quad (19)$$

for the number densities at heights larger than z_m .

3. Interpretation of results

In our first attempts to obtain a theoretical time-dependent model of the upper atmosphere properties by solving the heat conduction equation for the atmosphere in quasi-hydrostatic equilibrium (Eq 11-16)—a model which should represent the observed densities satisfactorily—we used as the only heat source the absorption of solar EUV-radiation combined, however, with the heat loss due to the infrared re-radiation by oxygen atoms. The loss due to re-radiation has only a small influence on the temperature distribution, as previously noted by D. C. Hunt and T. E. Van Zandt (1961). The source Q' in Eq 11 was taken equal to zero in these first attempts. The calculations yield a diurnal maximum of temperature and density at 17^h local time, not at 14^h as observed from satellite drag data. Losses due to conduction and infrared radiation by oxygen atoms are not sufficient to balance the heat input due

to the EUV-absorption in order to yield a maximum of temperature at 14^h local time. Furthermore, the ratio of daytime maximum temperature or density to nighttime minimum temperature or density, respectively, is much larger than the observed ratio. Our calculations using the EUV absorption as the only heat source yield a value of 2.6 for the temperature ratio, while the observed value is about 1.5. These results are qualitatively independent of boundary conditions. For testing we used two different sets of number densities which differ considerably in the important ratio of O to O₂ at the lower boundary. Diffusive equilibrium was assumed to be valid for all altitudes above 120 km. The numerical values for the boundary conditions at 120 km are given in Table 1.

TABLE 1. Boundary values at 120-km altitude.

	Set 1	Set 2
Number density: N ₂	5.80 × 10 ¹¹	5.95 × 10 ¹¹
Number density: O ₂	1.20 × 10 ¹¹	3.13 × 10 ¹⁰
Number density: O	7.60 × 10 ¹⁰	2.57 × 10 ¹¹
Number density: He	2.50 × 10 ⁷	2.50 × 10 ⁷
Number density: H	4.36 × 10 ⁴	4.36 × 10 ⁴
Temperature	355K	355K

In set 1 the values for N₂, O₂, O and He were taken from M. Nicolet (1961b) and the value for H was taken from R. Jastrow and L. Kyle (1961). In set 2 all values are from Jastrow and Kyle, except the He-value, which is the same as in set 1. A temperature of 355K at 120 km was chosen in both cases. No attempt was made to account for a diurnal variation of this temperature, as one does not expect any considerable variation at this altitude. However, a further investigation is desirable.

Mean values for the photoionization cross sections were used: 15, 15, 12 × 10⁻¹⁸ cm² for N₂, O₂ and O, respectively. These averages are valid for the wavelength range from about 60 Å to 900 Å.

The incident flux was chosen to yield a model which is in agreement with the average observed densities (temperatures), specifically around 600-km altitude. For illustration we present the maximum and minimum values for temperature and density at 600-km altitude for two different fluxes of the EUV-radiation. In the first example the flux was 1.8 erg cm⁻² sec⁻¹ and the first set of boundary values was used. We obtain a maximum temperature of 1959 degree K at 17^h local time, a minimum of 849K at 6^h local time. The corresponding densities are 1.59 × 10⁻¹⁵ gm cm⁻³ and 3.44 × 10⁻¹⁷ gm cm⁻³. In the second example the flux was 2.2 erg cm⁻² sec⁻¹ and the second set of boundary values was used. The maximum and minimum temperatures and densities obtained at 600 km are: 2026K at 17^h local time, 910K at 6^h local time, and 3.81 × 10⁻¹⁵ gm cm⁻³, 1.47 × 10⁻¹⁶ gm cm⁻³, respectively.

The peak fluxes are generally considerably higher than the flux of $1.1 \text{ erg cm}^{-2} \text{ sec}^{-1}$ required by D. C. Hunt and T. E. Van Zandt (1961), who compared the observed data at diurnal maximum with a time-independent solution. The explanation for the discrepancy is that the time-independent solution can only be applied to define diurnal average values if one considers the time-independent flux as a diurnal average. A comparison with the observed diurnal maximum values therefore yields unacceptable conclusions.

The diurnal variation of the temperature calculated with the EUV heat source only is given in Fig. 1 for an altitude of 600 km by the dotted line, together with the temperature distribution (solid line), which well represents the observed data.

Thus, it can be concluded that no agreement can be obtained between the observations and a theory which is based on an EUV heat source alone. Furthermore, an extremely high efficiency (70 to 90 per cent) would be required for the conversion of the EUV flux into thermospheric heat if we are to compare with Hinteregger's rocket measurements (H. E. Hinteregger, 1961) which yield a total flux of $2.5 \text{ erg cm}^{-2} \text{ sec}^{-1}$ in the range from 44 \AA to 1000 \AA .

Therefore, the existence of a second heat source with the following properties is strongly suggested: a maximum in the mid-morning and a minimum in the early or mid-afternoon, a small amount of heating

during the night, and an average magnitude comparable to the heat provided by the EUV flux.

A heat source with these properties is required to represent the density observed in those times where a strong diurnal bulge is found. For the comparison we used the model of Bonn Observatory 1961 (H. A. Martin *et al.*, 1961). This model is in very good agreement with the density data obtained by other groups. This model is reduced to years of high solar activity, represented by a 10.7 cm solar radiation flux of

$$S = 200 \times 10^{-22} \text{ Wm}^{-2} (\text{cps})^{-1}$$

or by the corresponding flux

$$S = 170 \times 10^{-22} \text{ Wm}^{-2} (\text{cps})^{-1}$$

of the 20-cm solar radiation.

The time variation of this new heat source, which we designated in the introduction as the "corpuscular" heat source, might be correlated with some other geomagnetic phenomena, which should be an indicator of corpuscular activity. The intensities of the micro-pulsations observed by W. H. Campbell (1959) in California show the main maximum at about 9^{h} local time, and thus have the principal property required. A physical connection of these pulsations with the heat source we found necessary is plausible, but direct observations of micropulsations in the ionospheric F -layer would be desirable. In addition the geomagnetic field strength at the equator also has approximately the time-varying properties required.

The diurnal variation of the flux for the corpuscular heat source which we have chosen is given in Fig. 2, together with the fraction of the solar EUV flux con-

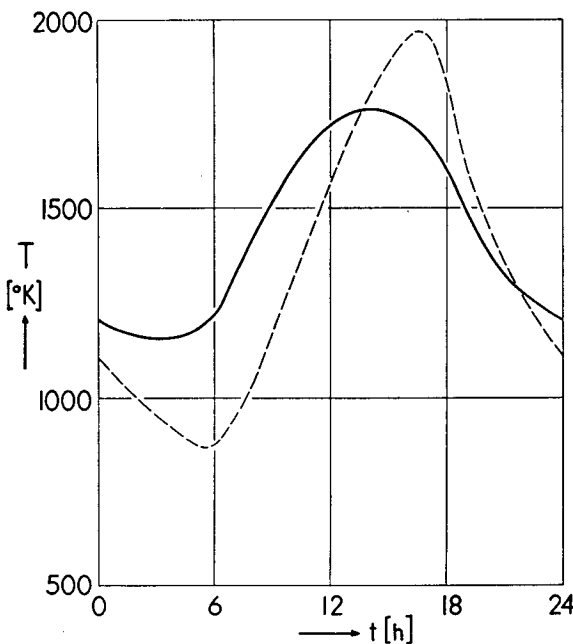


FIG. 1. Diurnal variation of the exospheric temperature calculated with an EUV-heat source alone (dotted curve) and combined with our additional "corpuscular" heat source (solid curve) as function of local time.

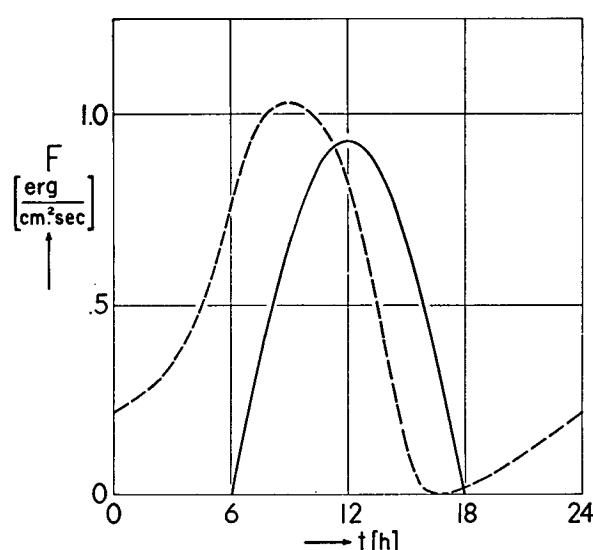


FIG. 2. Diurnal variation of the fluxes of the EUV-heat source (solid curve) and of the "corpuscular" heat source (dotted curve).

verted into heat in the thermosphere having a peak value of $0.93 \text{ erg cm}^{-2} \text{ sec}^{-1}$. This implies an efficiency factor of 37 per cent.

The peak value of the flux for the corpuscular heat source that yields a good agreement with the observed densities is $1.03 \text{ erg cm}^{-2} \text{ sec}^{-1}$. This value is in good agreement with the estimates obtained from the semi-annual variation (see introduction). It agrees also with the magnitude of the heat source proposed by J. Dessler (1959)—a source which is due to the dissipation of hydromagnetic waves generated by the solar corpuscular radiation. The energy dissipation takes place in the F region of the ionosphere. For the altitude dependence of our corpuscular heat source Q' we used an analytic approximation to the dissipation curve given by Dessler. This form is also similar to the shape of the heat source due to absorption of solar EUV radiation. Our expression for Q' is:

$$Q' = \frac{F}{s_1 - s_2} \left[\exp\left(-\frac{z-z_0}{s_1}\right) - \exp\left(-\frac{z-z_0}{s_2}\right) \right] f(t),$$

where F is the flux of this heat source

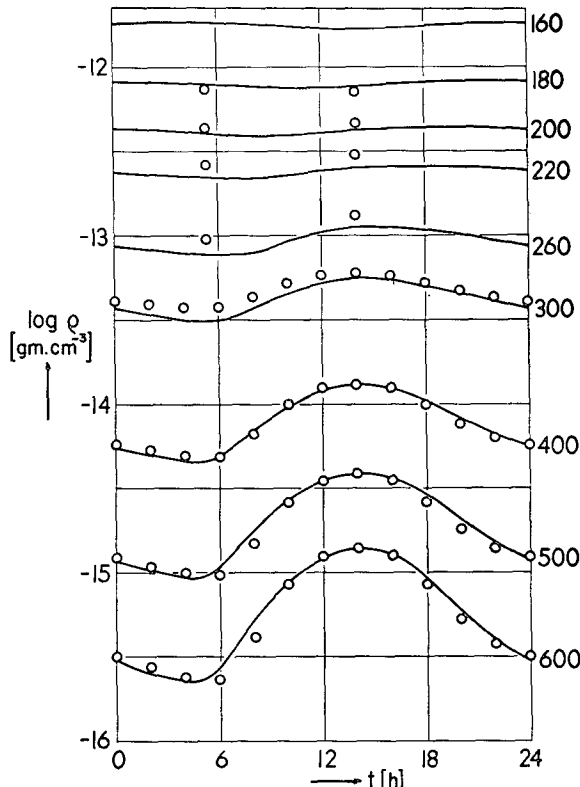


FIG. 3. Diurnal variation of density as function of local time for selected altitudes from 160 to 600 km. The solid curves give our calculated values. The circles are densities taken from the observational model of Bonn University Observatory 1961 (H. A. Martin *et al.*, 1961).

$$F = \int_{z_0}^{\infty} Q'(z, t_{MAX}) dz$$

at the time of its peak value with

$$s_1 = 60 \text{ km},$$

$$s_2 = 40 \text{ km},$$

$$z_0 = 120 \text{ km}.$$

$f(t)$ is the diurnal variation, normalized to a peak value equal to unity. It is represented by the following Fourier coefficients:

$$\begin{aligned} a_0 &= +0.427, & a_1 &= -0.263, & a_2 &= +0.063 \\ a_3 &= -0.015, & a_4 &= +0.024, & a_5 &= -0.006 \\ a_6 &= -0.004, & & & & \\ b_1 &= +0.369, & b_2 &= -0.156, & b_3 &= +0.010 \\ b_4 &= +0.208, & b_5 &= -0.007 & & \end{aligned}$$

The Q' -function has a maximum at 170 km.

Using this heat source in addition to the EUV heat source we obtained a good agreement between the observed and calculated densities. The best general agreement is obtained with the first set of boundary conditions (Table 1). The solid line in Fig. 1 shows the calculated diurnal variation of the exospheric temperature. In Figs. 3 and 4 the derived diurnal variations of densities are compared with the densities of the model

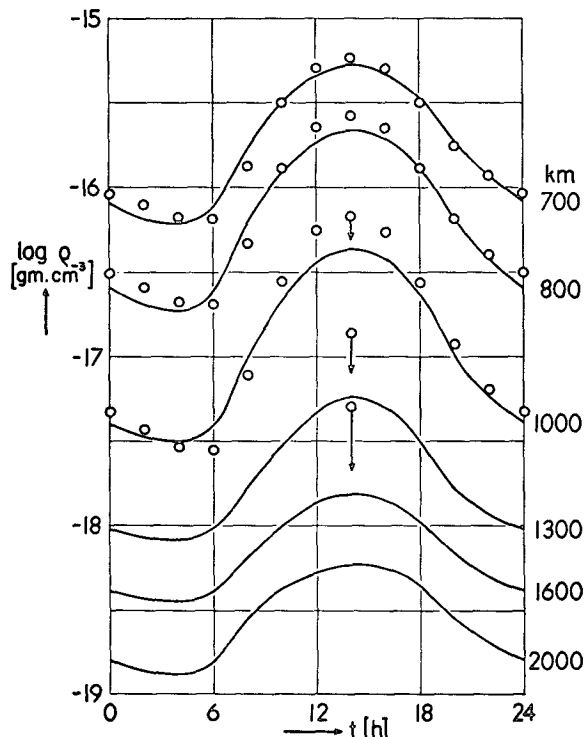


FIG. 4. Same as Fig. 3 for altitudes from 700 km to 2000 km.

of Bonn Observatory (H. A. Martin *et al.*, 1961). In the altitude range from 400 to 700 km, where the Bonn model is based on the most reliable density determinations, we have an almost perfect agreement. For altitudes below 400 km the agreement is also satisfactory. In the range above an altitude of 1000 km the Bonn Observatory model is based on densities derived from the satellite Echo I by M. Roemer (1961 a, b). Since his method for determining densities takes into account the diurnal bulge by considering how the orbit traverses the bulge, an auxiliary model was needed for his calculations. The one he used early in 1961 was based on an extrapolation of the altitude variation of the diurnal amplitude. This variation increased systematically with height. In an atmosphere containing a helium layer, where the mean molecular weight decreases with altitude and time, the amplitude of the diurnal density variations begins, however, to decrease again above 1000 km (see Fig. 4). Therefore, the maximum densities in the Bonn model for altitudes above 1000 km are too high by an estimated amount indicated by the arrows in Fig. 4. Those reduced densities are then in better agreement with our calculated densities. The densities determined by R. Bryant (1961) using a general density scale height of 260 km in his calculations are all well placed between our maximum and minimum density curves in the altitude range from 1057 km to 1450 km.

The temperature, scale height and mean molecular weight are given as functions of altitude for four selected local times of the day in Figs. 5, 6 and 7, respectively. It may be noticed that the 10^h- and the 22^h-temperature curves in Fig. 5 cross at about 170 km. This is related to the fact that the daytime-densities in the altitude range from 130 to 190 km are lower than the nighttime-densities. This is in agreement with the observational model by H. A. Martin *et al.* (1961). The mass difference between nighttime and daytime densities below 190 km is sufficient to provide the

mass for the diurnal bulge above that height, since our model conserves the total mass (see Eq 6).

In Fig. 8 we compare the densities of the observational model at an altitude of 600 km with the calculated densities using both sets of boundary conditions which differ considerably in the ratio of O to O₂ at 120 km. In general, both sets afford a satisfactory agreement in the range from 200 km to 600 km. It is seen in Fig. 8 that the first set yields a better fit with the observed data at 600 km. But the discrepancy is

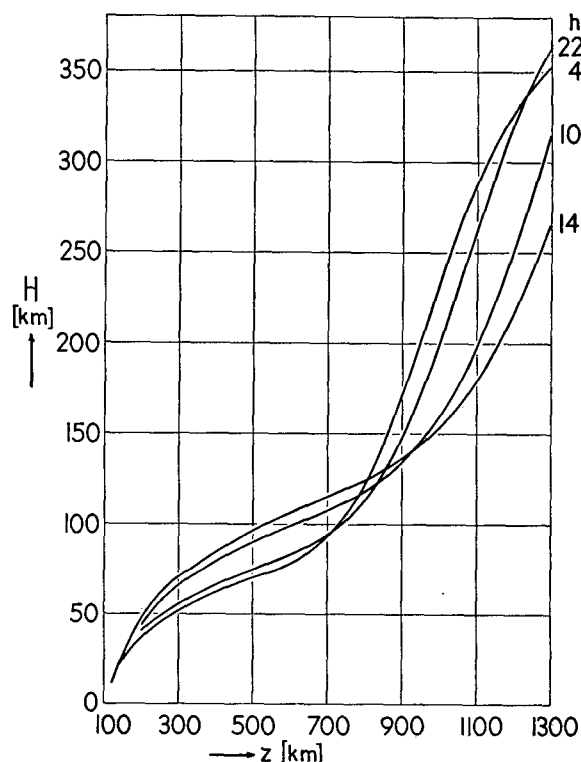


FIG. 6. The pressure scale heights as function of altitude from 120 km to 1300 km for four selected local times.

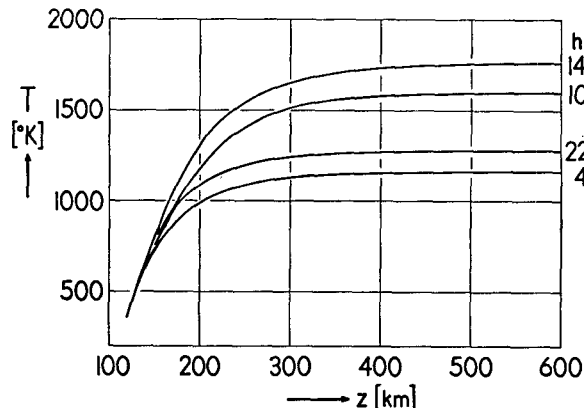


FIG. 5. Temperature (deg K) as function of altitude from 120 km to 600 km for four selected local times.

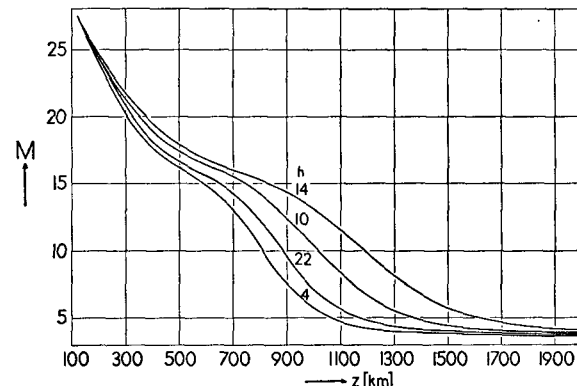


FIG. 7. The mean molecular weight as function of altitude from 120 km to 1300 km for four selected local times.

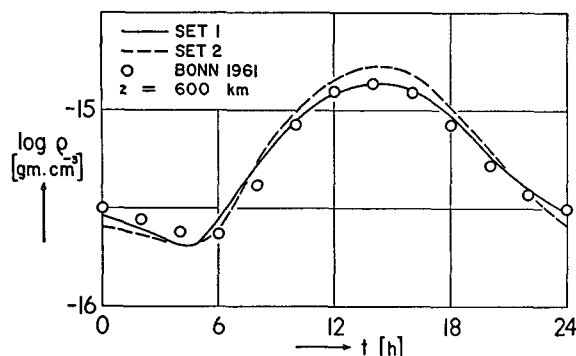


FIG. 8. Comparison of the calculated densities using the two sets of boundary conditions (Table 1) with the observed data of the Bonn Model 1961 at an altitude of 600 km.

not large enough definitely to rule out the second set. It may well be that the observed densities need some systematic corrections since the atmospheric bulge was taken into account only approximately in reducing the observational data (H. A. Martin *et al.*, 1961).

It is interesting to compare the exospheric maximum and minimum temperatures for these two sets of calculations. For the first set of boundary conditions they are: 1770K for the diurnal maximum and 1160K for the diurnal minimum. The corresponding temperatures for the second set are 1515K and 975K, respectively. This demonstrates how sensitive the exospheric temperature is to the boundary conditions, especially to the ratio of O to O₂. In the first set this ratio is 0.63; in the second set it is 8.2.

The physical properties of the upper atmosphere based on the first set of boundary conditions (Table 1) are given in the appendix tables as function of altitude from 120 km to 2050 km for selected hours in local time. The properties are listed in the following order: Temperature (deg K), density (gm cm⁻³), pressure (dyne cm⁻²), scale height (pressure scale height) (km), mean molecular weight and finally the number densities (cm⁻³) for N₂, O₂, O, He and H. At the beginning of each table the local time is given in hours. Further, the cosine of the zenith angle (theta) of the sun during the times of equinoxes on the equator and the temperature gradient (in deg K per km) (labeled Int Grad) at 120 km are given.

Our model pertains to the equatorial and temperate zones of the earth and is valid for those years when the solar activity can be represented by an average flux of 200×10^{-22} Wm⁻² (cps)⁻¹ for the 10.7-radiation (or a flux of 170×10^{-22} Wm⁻² (cps)⁻¹ for the 20-cm radiation).

We wish to emphasize again that to obtain a good agreement with the observational model a heat source in addition to the solar EUV flux is required. It is probable that this heat source derives its energy ultimately from the solar corpuscular radiation.

In our calculations we obtained good agreement with

the observational models with a flux having a diurnal average of $0.44 \text{ erg cm}^{-2} \text{ sec}^{-1}$ and a peak value of $1.03 \text{ erg cm}^{-2} \text{ sec}^{-1}$ at 9^h local time, combined with an EUV heat source having an average flux of $0.30 \text{ erg cm}^{-2} \text{ sec}^{-1}$ and a peak value of $0.93 \text{ erg cm}^{-2} \text{ sec}^{-1}$ at 12^h local time.

Of the four effects mentioned in the introduction, our calculated model covers only the diurnal variation. The three other effects could be represented by changes in the total fluxes of the two heat sources. Both are expected to vary considerably during the 11-yr solar cycle. The analysis of the density determinations from satellite drag measurements during an entire solar cycle could reveal the necessary information about the flux variations of the two heat sources. But we should also be prepared for the possibility that the diurnal variation of the corpuscular heat source may change in shape and in position of the maximum during the solar cycle. Therefore, direct measurements of the solar EUV radiation and of the solar wind intensity outside the magnetosphere for at least one solar cycle are urgently desired.

Acknowledgments. We are very much obliged to Dr. R. Jastrow for his stimulation and permanent interest. We would like to acknowledge our indebtedness to Mr. Lee Kyle and Dr. R. Jastrow for the development of the earlier phase of the program from which our procedure was derived. Further, we wish to express our very great appreciation to Mr. E. Monasterski for preparation of the extensive machine program and the construction of the procedure for numerical integration of the conduction equations. We are also grateful to Mr. L. Lefton for his assistance in running the program.

REFERENCES

- Bartels, J., 1932: Terrestrial-magnetic activity and its relations to solar phenomena. *Terr. Magn.*, **37**, 1-52.
- Bates, D. R., 1951: The temperature of the upper atmosphere. *Proc. Royal Soc. London*, Sect. B **64**, 805-821.
- Bridge, H. S., C. Dilworth, A. J. Lazarus, C. F. Lyon, B. Rossi and F. Scherb, 1961: Direct observations of the interplanetary plasma. *Lab. Nucl. Sci. and Dep. Phys. M.I.T. Preliminary Rep.*, 13 pp.
- Bryant, R., 1961: A comparison of theory and observation of the Echo I satellite. *J. geophys. Res.*, **66**, 3066-3069.
- Campbell, W. H., 1959: Studies of magnetic field micropulsations with periods of 5 to 30 seconds. *J. geophys. Res.*, **64**, 1819-1826.
- Chapman, S., and T. G. Cowling, 1960: *The mathematical theory of non-uniform gases*. Cambridge, University Press, 431 pp.
- Cortie, A. L., 1912: Sunspots and terrestrial magnetic phenomena, 1898-1911. *Monthly Notices*, **73**, 52-60.
- Dessler, A. J., 1959: Ionospheric heating by hydromagnetic waves. *J. geophys. Res.*, **64**, 397-401.
- Diaz, G. B., R. S. Clippinger, B. Friedman, E. Isaacson and R. Richtmyer, 1958: Partial differential equations. *Handbook of automation, computation and control*, Vol. 1, New York, Pergamon Press, Sect. 14, pp. 64-90.
- Eckart, C., 1960: *Hydrodynamics of oceans and atmospheres*. New York, Pergamon Press, 290 pp.
- Groves, G. V., 1961: Correlation of upper atmosphere air density with geomagnetic activity, November 1960. *Space research*, **2**, Amsterdam, North Holland Publ. Co., 751-753.

- Hinteregger, H. E., 1961: Preliminary data on solar extreme ultraviolet radiation in the upper atmosphere. *J. geophys. Res.*, **66**, 2367-2380.
- Hunt, D. C., and T. E. Van Zandt, 1961: Photoionization heating in the F-region of the atmosphere. *J. geophys. Res.*, **66**, 1673-1682.
- Jacchia, L. G., 1959a: Atmospheric fluctuations of solar origin revealed by satellites. Harvard Observatory Announcement Card No. 1423.
- , 1959b: Solar effects on the acceleration of artificial satellites. Smithsonian Astrophys. Obs. Spec. Rep. No. 29, 15 pp.
- , 1959c: Corpuscular radiation and the acceleration of the artificial satellites. *Nature*, **183**, 1662-1663.
- , 1960: A variable atmospheric-density model from satellite accelerations. Smithsonian Astrophys. Obs. Spec. Rep. No. 39, 15 pp.
- , 1961a: Satellite drag during the events of November 1960. *Space research*, **2**, Amsterdam, North Holland Publ. Co., 747-750.
- , 1961b: A working model of the upper atmosphere. *Nature*, **192**, 1147-1148.
- , and J. Slowey, 1962: Preliminary analysis of the atmospheric drag of the twelve-foot balloon satellite (1961 delta 1). Smithsonian Astrophys. Obs. Spec. Rep. No. 84, 18 pp.
- Jastrow, R., and R. Bryant, 1961: Effects of a severe solar storm on the orbit of Echo I. *IGY Bulletin*, **44**, 6-7.
- Jastrow, R., and L. Kyle, 1961: The earth atmosphere. *Handbook of astronautical engineering*, New York, Toronto, London, McGraw-Hill, Sect. 2, pp. 2-13.
- King-Hele, D. G., and D. M. C. Walker, 1961: Upper-atmosphere density during the years 1957-1961 determined from satellite orbits. *Space research*, **2**, Amsterdam, North Holland Publ. Co., 918-957.
- Lowan, A. N., 1955: On the cooling of the upper atmosphere after sunset. *J. geophys. Res.*, **60**, 421-429.
- Martin, H. A., W. Neveling, W. Priester and M. Roemer, 1961: Model of the upper atmosphere from 130 through 1600 km derived from satellite orbits. Mitt. Sternwarte Bonn No. 35, 16 pp.; and *Space research*, **2**, Amsterdam, North Holland Publ. Co., 902-917.
- Nicolet, M., 1960: Les variations de la densité et du transport de chaleur par conduction dans l'atmosphère supérieure. *Space research*, **1**, Amsterdam, North Holland Publ. Co., 46-89.
- , 1961a: Structure of the thermosphere. *Planetary Space Sci.*, **5**, 1-32.
- , 1961b: Density of the heterosphere related to temperature. *Res. in Space Sci.*, Smithsonian Inst. Astrophys. Observ., Spec. Rpt. 75, 30 pp.
- Paetzold, H. K., 1959: Observations of the Russian satellites and the structure of the outer terrestrial atmosphere. *Planetary Space Sci.*, **1**, 115-124.
- , 1960: Proceedings XI Internat. Astronautical Congress, Stockholm. (in press).
- , and H. Zschoerner, 1960: Bearings of Sputnik III and the variable acceleration of satellites. *Space research*, **1**, Amsterdam, North Holland Publ. Co., 24-36.
- , 1961: The structure of the upper atmosphere and its variations after satellite observations. *Space research*, **2**, Amsterdam, North Holland Publ. Co., 958-973.
- Priester, W., 1959: Sonnenaktivität und Abbremsung der Erd-satelliten. Mitt. Univ. Sternwarte Bonn, No. 24, 4 pp.; and *Naturwissenschaften*, **46**, 197-198.
- , 1961: Solar activity effect and diurnal variation in the upper atmosphere. *J. geophys. Res.*, **66**, 4143-4148.
- , and H. A. Martin, 1960: Solare und tageszeitliche Effekte in der Hochatmosphäre aus Beobachtungen künstlicher Erdsatelliten. Mitt. Univ. Bonn No. 29, 53 pp. Engl. translation: Royal Aircraft Establishment Farnborough Library translation No. 901, 20 pp.
- , —, and K. Kramp, 1960: Diurnal and seasonal density variations in the upper atmosphere. *Nature*, **188**, 202-204.
- Priester, W., and D. Cattani, 1962: On the semiannual variation of geomagnetic activity and its relation to the solar corpuscular radiation. *J. atmos. Sci.*, **19**, 121-126.
- Ratcliffe, J. A., and K. Weekes, 1960: The ionosphere. *Physics of the upper atmosphere*, New York, London, Academic Press, 377-470.
- Roemer, M., 1961a: Modell der Exosphäre im Höhenbereich 1000-1700 km. berechnet aus den Bahnderungen des Satelliten Echo 1. Mitt. Univ. Sternwarte Bonn No. 37, 34 pp. Engl. translation: Royal Aircraft Establishment, Farnborough. Library translation No. 954, 32 pp.
- , 1961b: Terrestrial exosphere at heights of 1000-1700 km. *Nature*, **191**, 238-240.
- Spitzer, L., 1949: The terrestrial atmosphere above 300 km. *The atmospheres of the earth and planets*, revised edition, 1952, Chicago, Univ. of Chicago Press, 211-247.
- Waldmeier, M., and H. Mueller, 1950: Die Sonnenstrahlung im Gebiet von $\lambda=10$ cm. *Z. Astrophys.*, **27**, 58-66.
- Zadunaisky, P. E., I. I. Shapiro and H. M. Jones, 1961: Experimental and theoretical results on the orbit of Echo 1. Smithsonian Astrophys. Obs. Spec. Rep. No. 61, 22 pp.

APPENDIX

The properties of the upper atmosphere as functions of local time for selected hours of the day and as functions of altitude from 120 km to 2050 km

The model pertains to the equatorial and temperate zones of the earth when the average solar activity is represented by a solar radiation flux of 200×10^{-22} $\text{Wm}^{-2} (\text{cps})^{-1}$ at 10.7-cm wavelength.

The listed quantities are:

- Temperature (deg K)
- Density (gm cm^{-3})
- Pressure (dynes cm^{-2})
- Scale height (km)
- Mean molecular weight
- Number densities (cm^{-3}) for N_2 , O_2 , O, He, H.

Powers of 10 are indicated by the number following the letter E (for example, $3.536E-11 \equiv 3.536 \times 10^{-11}$).

Computations for all 24 hours have been made; to save space only 5 selected hours are reproduced herein.

TABLE 2. Properties of the upper atmosphere for 4.000^h local time as a function of altitude from 120 to 2050 km
(cosθ = 5.0000E-01, Int grad = 1.7032E 01).

Alt km	Temp K	Density gm cm ⁻³	Pressure dyne cm ⁻²	Scale ht km	Mean mol wt	N(N ₂) cm ⁻³	N(O ₂) cm ⁻³	N(O) cm ⁻³	N(He) cm ⁻³	N(H) cm ⁻³
120	355	3.536E-11	3.802E-02	11.4	27.46	5.800E 11	1.200E 11	7.600E 10	2.500E 07	4.356E 04
130	509	1.181E-11	1.855E-02	16.7	26.98	1.931E 11	3.598E 10	3.471E 10	1.567E 07	2.956E 04
140	632	5.516E-12	1.091E-02	21.1	26.55	9.839E 10	1.539E 10	2.038E 10	1.167E 07	2.337E 04
150	728	3.046E-12	7.051E-03	24.7	26.14	4.876E 10	7.861E 09	1.356E 10	9.472E 06	1.994E 04
160	804	1.856E-12	4.820E-03	27.8	25.74	2.928E 10	4.452E 09	9.705E 09	8.083E 06	1.779E 04
170	865	1.206E-12	3.421E-03	30.5	25.34	1.869E 10	2.694E 09	7.276E 09	7.119E 06	1.632E 04
180	914	8.189E-13	2.496E-03	32.9	24.94	1.244E 10	1.706E 09	5.630E 09	6.404E 06	1.525E 04
190	954	5.747E-13	1.858E-03	35.0	24.53	8.534E 09	1.116E 09	4.455E 09	5.847E 06	1.443E 04
200	987	4.136E-13	1.407E-03	36.9	24.13	5.988E 09	7.485E 08	3.585E 09	5.397E 06	1.379E 04
220	1038	2.267E-13	8.387E-04	40.4	23.31	3.093E 09	3.545E 08	2.406E 09	4.705E 06	1.284E 04
240	1073	1.314E-13	5.207E-04	43.5	22.50	1.670E 09	1.762E 08	1.667E 09	4.186E 06	1.216E 04
260	1097	7.944E-14	3.337E-04	46.4	21.72	9.292E 08	9.051E 07	1.180E 09	3.773E 06	1.165E 04
280	1115	4.966E-14	2.196E-04	49.1	20.96	5.279E 08	4.755E 07	8.484E 08	3.432E 08	1.124E 04
300	1127	3.192E-14	1.477E-04	51.7	20.26	3.045E 08	2.541E 07	6.164E 08	3.141E 06	1.090E 04
320	1136	2.101E-14	1.012E-04	54.2	19.61	1.776E 08	1.375E 07	4.513E 08	2.888E 06	1.061E 04
340	1142	1.412E-14	7.052E-05	56.5	19.03	1.046E 08	7.512E 06	3.325E 08	2.663E 06	1.036E 04
360	1147	9.667E-15	4.983E-05	58.7	18.50	6.200E 07	4.138E 06	2.462E 08	1.013E 04	
380	1150	6.723E-15	3.564E-05	60.7	18.04	3.698E 07	2.295E 06	1.829E 08	2.280E 06	9.911E 03
400	1153	4.741E-15	2.577E-05	62.6	17.64	2.217E 07	1.280E 06	1.364E 08	2.115E 06	9.710E 03
420	1155	3.385E-15	1.881E-05	64.4	17.28	1.335E 07	7.173E 05	1.020E 08	1.963E 06	9.520E 03
440	1156	2.442E-15	1.384E-05	66.0	16.96	8.073E 06	4.039E 05	7.643E 07	1.825E 06	9.339E 03
460	1157	1.779E-15	1.026E-05	67.6	16.68	4.900E 06	2.284E 05	5.742E 07	1.697E 06	9.165E 03
480	1158	1.306E-15	7.659E-06	69.2	16.42	2.984E 06	1.297E 05	4.323E 07	1.579E 06	8.997E 03
500	1159	9.659E-16	5.753E-06	70.7	16.17	1.824E 06	7.389E 04	3.261E 07	1.471E 06	8.835E 03
520	1159	7.188E-16	4.348E-06	72.2	15.93	1.118E 06	4.226E 04	2.464E 07	1.370E 06	8.677E 03
540	1160	5.380E-16	3.305E-06	73.7	15.70	6.875E 05	2.426E 04	1.866E 07	1.278E 06	8.524E 03
560	1160	4.048E-16	2.527E-06	75.3	15.45	4.241E 05	1.397E 04	1.415E 07	1.192E 06	8.375E 03
580	1160	3.060E-16	1.944E-06	77.1	15.19	2.624E 05	8.075E 03	1.075E 07	1.112E 06	8.229E 03
600	1161	2.324E-16	1.504E-06	79.1	14.90	1.628E 05	4.682E 03	8.180E 06	1.038E 06	8.088E 03
620	1161	1.772E-16	1.172E-06	81.2	14.59	1.013E 05	2.724E 03	6.235E 06	9.694E 05	7.949E 03
640	1161	1.357E-16	9.195E-07	83.7	14.25	6.321E 04	1.590E 03	4.760E 06	9.058E 05	7.814E 03
660	1161	1.044E-16	7.268E-07	86.5	13.87	3.955E 04	9.308E 02	3.640E 06	8.467E 05	7.683E 03
680	1161	8.065E-17	5.791E-07	89.7	13.45	2.482E 04	5.467E 02	2.788E 06	7.917E 05	7.554E 03
700	1162	6.260E-17	4.653E-07	93.4	12.99	1.562E 04	3.221E 02	2.139E 06	7.407E 05	7.428E 03
720	1162	4.882E-17	3.774E-07	97.6	12.50	9.851E 03	1.903E 02	1.643E 06	6.932E 05	7.306E 03
740	1162	3.828E-17	3.090E-07	102.5	11.97	6.232E 03	1.128E 02	1.265E 06	6.490E 05	7.186E 03
760	1162	3.018E-17	2.555E-07	108.2	11.41	3.952E 03	6.707E 01	9.745E 05	6.078E 05	7.068E 03
780	1162	2.394E-17	2.135E-07	114.6	10.84	2.513E 03	4.000E 01	7.521E 05	5.695E 05	6.954E 03
800	1162	1.912E-17	1.802E-07	121.8	10.25	1.602E 03	2.392E 01	5.813E 05	5.338E 05	6.842E 03
820	1162	1.537E-17	1.537E-07	129.9	9.67	1.024E 03	1.435E 01	4.500E 05	5.005E 05	6.732E 03
840	1162	1.246E-17	1.324E-07	138.9	9.09	6.561E 02	8.630E 00	3.488E 05	4.695E 05	6.625E 03
860	1162	1.018E-17	1.152E-07	148.7	8.54	4.214E 02	5.206E 00	2.708E 05	4.405E 05	6.520E 03
880	1162	8.386E-18	1.012E-07	159.4	8.01	2.714E 02	3.149E 00	2.105E 05	4.135E 05	6.418E 03
900	1162	6.972E-18	8.963E-08	170.7	7.52	1.752E 02	1.910E 00	1.639E 05	3.883E 05	6.317E 03
920	1163	5.851E-18	8.003E-08	182.7	7.07	1.134E 02	1.162E 00	1.278E 05	3.648E 05	6.219E 03
940	1163	4.956E-18	7.199E-08	195.0	6.65	7.353E 01	7.089E 01	9.973E 04	3.428E 05	6.123E 03
960	1163	4.238E-18	6.518E-08	207.6	6.29	4.781E 01	4.336E-01	7.796E 04	3.222E 05	6.029E 03
980	1163	3.659E-18	5.936E-08	220.3	5.96	3.116E 01	2.659E-01	6.103E 04	3.030E 05	5.937E 03
1000	1163	3.187E-18	5.434E-08	232.8	5.67	2.035E 01	1.635E-01	4.783E 04	2.850E 05	5.847E 03
1050	1163	2.342E-18	4.440E-08	262.3	5.10	7.090E 00	4.905E-02	2.617E 04	2.449E 05	5.630E 03
1100	1163	1.802E-18	3.703E-08	288.1	4.70	2.505E 00	1.495E-02	1.443E 04	2.109E 05	5.423E 03
1150	1163	1.438E-18	3.133E-08	309.6	4.44	8.974E-01	4.630E-03	8.021E 03	1.820E 05	5.227E 03
1200	1163	1.179E-18	2.678E-08	327.0	4.26	3.259E-01	1.456E-03	4.494E 03	1.574E 05	5.040E 03
1250	1163	9.862E-19	2.306E-08	341.2	4.13	1.199E-01	4.649E-04	2.536E 03	1.363E 05	4.862E 03
1300	1163	8.365E-19	1.996E-08	352.9	4.05	4.471E-02	1.507E-04	1.442E 03	1.183E 05	4.693E 03
1350	1163	7.166E-19	1.736E-08	362.8	3.99	1.688E-02	4.955E-05	8.263E 02	1.029E 05	4.532E 03
1400	1163	6.184E-19	1.515E-08	371.7	3.95	6.455E-03	1.653E-05	4.768E 02	8.959E 04	4.378E 03
1450	1163	5.366E-19	1.326E-08	379.9	3.91	2.499E-03	5.593E-06	2.770E 02	7.817E 04	4.231E 03
1500	1163	4.676E-19	1.164E-08	387.6	3.88	9.791E-04	1.918E-06	1.621E 02	6.833E 04	4.091E 03
1550	1163	4.088E-19	1.025E-08	395.2	3.86	3.882E-04	6.670E-07	9.548E 01	5.982E 04	3.957E 03
1600	1163	3.584E-19	9.041E-09	402.7	3.83	1.557E-04	2.350E-07	5.662E 01	5.246E 04	3.830E 03
1650	1163	3.150E-19	7.994E-09	410.3	3.81	6.316E-05	8.387E-08	3.379E 01	4.609E 04	3.708E 03
1700	1163	2.774E-19	7.085E-09	418.0	3.78	2.591E-05	3.032E-08	2.030E 01	4.055E 04	3.591E 03
1750	1163	2.448E-19	6.293E-09	425.9	3.76	1.075E-05	1.110E-08	1.227E 01	3.573E 04	3.479E 03
1800	1163	2.165E-19	5.602E-09	434.0	3.74	4.506E-06	4.113E-09	7.462E 00	3.154E 04	3.372E 03
1850	1163	1.918E-19	4.998E-09	442.4	3.71	1.909E-06	1.543E-09	4.566E 00	2.788E 04	3.270E 03
1900	1163	1.702E-19	4.469E-09	451.2	3.68	8.174E-07	5.857E-10	2.811E 00	2.468E 04	3.172E 03
1950	1163	1.514E-19	4.005E-09	460.3	3.65	3.536E-07	2.249E-10	1.740E 00	2.188E 04	3.078E 03
2000	1163	1.348E-19	3.596E-09	469.7	3.62	1.545E-07	8.736E-11	1.084E 00	1.943E 04	2.987E 03
2050	1163	1.202E-19	3.237E-09	479.6	3.59	6.815E-08	3.432E-11	6.785E-01	1.727E 04	2.901E 03

TABLE 3. Properties of the upper atmosphere for 10.000^b local time as a function of altitude from 120 to 2050 km ($\cos\theta = -8.6602E-01$, Int grad = $1.6338E-01$).

Alt km	Temp K	Density gm cm ⁻³	Pressure dyne cm ⁻²	Scale ht km	Mean mol wt	N(N ₂) cm ⁻³	N(O ₂) cm ⁻³	N(O) cm ⁻³	N(He) cm ⁻³	N(H) cm ⁻³
120	355	3.536E-11	3.802E-02	11.4	27.46	5.800E 11	1.200E 11	7.600E 10	2.500E 07	4.356E 04
130	504	1.188E-11	1.846E-02	16.5	26.98	1.942E 11	3.616E 10	3.498E 10	1.582E 07	2.986E 04
140	629	5.489E-12	1.081E-02	21.0	26.54	8.893E 10	1.529E 10	2.036E 10	1.170E 07	2.347E 04
150	741	2.972E-12	7.003E-03	25.2	26.13	4.757E 10	7.660E 09	1.327E 10	9.297E 06	1.959E 04
160	845	1.776E-12	4.847E-03	29.2	25.75	2.803E 10	4.266E 09	9.266E 09	7.699E 06	1.693E 04
170	941	1.140E-12	3.516E-03	33.2	25.37	1.770E 10	2.563E 09	6.803E 09	6.571E 06	1.501E 04
180	1029	7.728E-13	2.642E-03	36.9	25.01	1.179E 10	1.631E 09	5.190E 09	5.744E 06	1.358E 04
190	1107	5.467E-13	2.039E-03	40.3	24.66	8.180E 09	1.086E 09	4.082E 09	5.120E 06	1.249E 04
200	1175	4.000E-13	1.607E-03	43.6	24.33	5.865E 09	7.492E 08	3.288E 09	4.635E 06	1.165E 04
220	1287	2.311E-13	1.045E-03	49.3	23.67	3.240E 09	3.855E 08	2.253E 09	3.938E 06	1.044E 04
240	1370	1.436E-13	7.105E-04	54.3	23.04	1.916E 09	2.134E 08	1.624E 09	3.446E 06	9.647E 03
260	1432	9.395E-14	4.987E-04	58.6	22.43	1.186E 09	1.241E 08	1.211E 09	3.111E 06	9.091E 03
280	1476	6.378E-14	3.584E-04	62.5	21.84	7.569E 08	7.469E 07	9.245E 08	2.841E 06	8.684E 03
300	1509	4.453E-14	2.625E-04	65.9	21.28	4.941E 08	4.603E 07	7.176E 08	2.623E 06	8.374E 03
320	1533	3.178E-14	1.952E-04	69.1	20.75	3.277E 08	2.887E 07	5.637E 08	2.440E 06	8.129E 03
340	1550	2.310E-14	1.470E-04	72.0	20.25	2.200E 08	1.834E 07	4.466E 08	2.282E 06	7.928E 03
360	1562	1.704E-14	1.119E-04	74.7	19.78	1.490E 08	1.177E 07	3.562E 08	2.143E 06	7.758E 03
380	1571	1.274E-14	8.603E-05	77.3	19.34	1.016E 08	7.610E 06	2.855E 06	2.019E 06	7.609E 03
400	1578	9.628E-15	6.670E-05	79.8	18.94	6.973E 07	4.952E 06	2.297E 08	1.905E 06	7.476E 03
420	1583	7.350E-15	5.210E-05	82.1	18.57	4.806E 07	3.239E 06	1.854E 08	1.801E 06	7.355E 03
440	1587	5.662E-15	4.097E-05	84.3	18.23	3.326E 07	2.128E 06	1.500E 08	1.705E 06	7.242E 03
460	1589	4.396E-15	3.242E-05	86.5	17.92	2.309E 07	1.403E 06	1.217E 08	1.616E 06	7.136E 03
480	1591	3.438E-15	2.579E-05	88.5	17.64	1.608E 07	9.286E 05	9.889E 07	1.532E 06	7.035E 03
500	1593	2.706E-15	2.062E-05	90.4	17.38	1.123E 07	6.165E 05	8.050E 07	1.454E 06	6.938E 03
520	1594	2.143E-15	1.657E-05	92.2	17.14	7.867E 06	4.105E 05	6.564E 07	1.381E 06	6.845E 03
540	1595	1.706E-15	1.337E-05	94.0	16.93	5.523E 06	2.741E 05	5.360E 07	1.312E 06	6.755E 03
560	1596	1.365E-15	1.083E-05	95.7	16.73	3.886E 06	1.835E 05	4.383E 07	1.246E 06	6.667E 03
580	1597	1.097E-15	8.801E-06	97.4	16.54	2.741E 06	1.232E 05	3.589E 07	1.185E 06	6.581E 03
600	1597	8.847E-16	7.180E-06	99.1	16.36	1.937E 06	8.287E 04	2.942E 07	1.127E 06	6.498E 03
620	1597	7.164E-16	5.877E-06	100.7	16.19	1.372E 06	5.590E 04	2.415E 07	1.072E 06	6.416E 03
640	1598	5.821E-16	4.827E-06	102.4	16.02	9.741E 05	3.779E 04	1.985E 07	1.021E 06	6.336E 03
660	1598	4.746E-16	3.976E-06	104.1	15.86	6.928E 05	2.561E 04	1.633E 07	9.718E 05	6.258E 03
680	1598	3.880E-16	3.286E-06	105.8	15.69	4.938E 05	1.740E 04	1.346E 07	9.255E 05	6.182E 03
700	1599	3.181E-16	2.725E-06	107.6	15.52	3.526E 05	1.184E 04	1.110E 07	8.817E 05	6.107E 03
720	1599	2.615E-16	2.266E-06	109.5	15.34	2.523E 05	8.082E 03	9.163E 06	8.402E 05	6.033E 03
740	1599	2.155E-16	1.891E-06	111.4	15.16	1.809E 05	5.527E 03	7.574E 06	8.009E 05	5.961E 03
760	1599	1.781E-16	1.583E-06	113.5	14.96	1.299E 05	3.788E 03	6.268E 06	7.637E 05	5.890E 03
780	1599	1.475E-16	1.329E-06	115.8	14.75	9.350E 04	2.601E 03	5.192E 06	7.284E 05	5.820E 03
800	1599	1.224E-16	1.120E-06	118.2	14.53	6.741E 04	1.791E 03	4.306E 06	6.949E 05	5.751E 03
820	1600	1.019E-16	9.478E-07	120.9	14.29	4.869E 04	1.235E 03	3.575E 06	6.631E 05	5.684E 03
840	1600	8.495E-17	8.048E-07	123.8	14.04	3.524E 04	8.536E 02	2.971E 06	6.330E 05	5.618E 03
860	1600	7.101E-17	6.860E-07	126.9	13.77	2.554E 04	5.912E 02	2.472E 06	6.044E 05	5.554E 03
880	1600	5.950E-17	5.872E-07	130.4	13.48	1.855E 04	4.103E 02	2.058E 06	5.772E 05	5.490E 03
900	1600	4.998E-17	5.048E-07	134.2	13.17	1.350E 04	2.854E 02	1.716E 06	5.514E 05	5.427E 03
920	1600	4.209E-17	4.359E-07	138.3	12.84	9.838E 03	1.989E 02	1.432E 06	5.269E 05	5.366E 03
940	1600	3.553E-17	3.781E-07	142.9	12.50	7.183E 03	1.388E 02	1.196E 06	5.036E 05	5.306E 03
960	1600	3.008E-17	3.295E-07	147.9	12.14	5.253E 03	9.714E 01	1.000E 06	4.815E 05	5.246E 03
980	1600	2.553E-17	2.885E-07	153.4	11.77	3.849E 03	6.809E 01	8.370E 05	4.604E 05	5.188E 03
1000	1600	2.174E-17	2.538E-07	159.4	11.39	2.824E 03	4.783E 01	7.013E 05	4.404E 05	5.131E 03
1050	1600	1.474E-17	1.884E-07	176.8	10.41	1.313E 03	1.994E 01	4.524E 05	3.945E 05	4.991E 03
1100	1600	1.021E-17	1.442E-07	198.0	9.42	6.164E 02	8.409E 00	2.936E 05	3.539E 05	4.858E 03
1150	1600	7.242E-18	1.136E-07	222.9	8.48	2.923E 02	3.587E 00	1.916E 05	3.179E 05	4.729E 03
1200	1600	5.270E-18	9.197E-08	251.3	7.62	1.400E 02	1.548E 00	1.258E 05	2.860E 05	4.606E 03
1250	1600	3.940E-18	7.623E-08	282.3	6.88	6.772E 01	6.753E-01	8.299E 04	2.577E 05	4.487E 03
1300	1600	3.027E-18	6.446E-08	314.9	6.25	3.306E 01	2.978E-01	5.507E 04	2.325E 05	4.373E 03
1350	1600	2.388E-18	5.542E-08	347.6	5.73	1.629E 01	1.327E-01	3.674E 04	2.100E 05	4.263E 03
1400	1600	1.932E-18	4.830E-08	379.4	5.32	8.103E 00	5.977E-02	2.464E 04	1.900E 05	4.158E 03
1450	1600	1.598E-18	4.255E-08	409.2	5.00	4.066E 00	2.719E-02	1.660E 04	1.720E 05	4.056E 03
1500	1600	1.348E-18	3.780E-08	436.5	4.74	2.058E 00	1.250E-02	1.125E 04	1.560E 05	3.958E 03
1550	1600	1.156E-18	3.382E-08	461.0	4.55	1.051E 00	5.800E-03	7.657E 03	1.416E 05	3.864E 03
1600	1600	1.006E-18	3.042E-08	482.8	4.40	5.409E-01	2.718E-03	5.238E 03	1.288E 05	3.773E 03
1650	1600	8.847E-19	2.748E-08	502.1	4.28	2.808E-01	1.285E-03	3.600E 03	1.172E 05	3.685E 03
1700	1600	7.854E-19	2.492E-08	519.2	4.19	1.470E-01	6.137E-04	2.486E 03	1.068E 05	3.600E 03
1750	1600	7.024E-19	2.266E-08	534.6	4.12	7.754E-02	2.957E-04	1.724E 03	9.741E 04	3.518E 03
1800	1600	6.319E-19	2.067E-08	548.5	4.07	4.123E-02	1.437E-04	1.201E 03	8.896E 04	3.439E 03
1850	1600	5.713E-19	1.889E-08	561.3	4.02	2.209E-02	7.049E-05	8.407E 02	8.133E 04	3.363E 03
1900	1600	5.185E-19	1.729E-08	573.2	3.99	1.193E-02	3.487E-05	5.909E 02	7.444E 04	3.290E 03
1950	1600	4.721E-19	1.586E-08	584.5	3.96	6.487E-03	1.739E-05	4.171E 02	6.820E 04	3.218E 03
2000	1600	4.310E-19	1.457E-08	595.2	3.93	3.554E-03	8.749E-06	2.956E 02	6.255E 04	3.150E 03
2050	1600	3.944E-19	1.341E-08	605.7	3.91	1.961E-03	4.437E-06	2.104E 02	5.743E 04	3.083E 03

TABLE 4. Properties of the upper atmosphere for 14,000^b local time as a function of altitude from 120 to 2050 km
(cosθ = -8.6603E-01, Int grad = 1.6315E 01).

Alt km	Temp K	Density gm cm ⁻³	Pressure dyne cm ⁻²	Scale ht km	Mean mol wt	N(N ₂) cm ⁻³	N(O ₂) cm ⁻³	N(O) cm ⁻³	N(He) cm ⁻³	(NH) cm ⁻³
120	355	3.536E-11	3.802E-02	11.4	27.46	5.800E 11	1.200E 11	7.600E 10	2.500E 07	4.356E 04
130	509	1.180E-11	1.849E-02	16.6	26.98	1.928E 11	3.591E 10	3.470E 10	1.568E 07	2.960E 04
140	652	5.365E-12	1.095E-02	21.7	26.55	8.695E-10	1.498E-10	1.979E 10	1.131E 07	2.265E 04
150	789	2.889E-12	7.241E-03	26.8	26.17	4.630E 10	7.495E 09	1.272E 10	8.777E 06	1.843E 04
160	916	1.742E-12	5.138E-03	31.6	25.81	2.755E 10	4.231E 09	8.866E 09	7.168E 06	1.566E 04
170	1030	1.137E-12	3.824E-03	36.1	25.47	1.774E 10	2.602E 09	6.554E 09	6.085E 06	1.376E 04
180	1130	7.876E-13	2.943E-03	40.3	25.15	1.210E 10	1.703E 09	5.059E 09	5.138E 06	1.241E 04
190	1218	5.697E-13	2.322E-03	44.1	24.84	8.610E 09	1.167E 09	4.034E 09	4.751E 06	1.141E 04
200	1293	4.261E-13	1.867E-03	47.5	24.54	6.329E 09	8.285E 08	3.297E 09	4.318E 06	1.065E 04
220	1413	2.562E-13	1.257E-03	53.5	23.96	3.667E 09	4.499E 08	2.323E 09	3.700E 06	9.585E 03
240	1502	1.648E-13	8.799E-04	58.6	23.39	2.263E 09	2.616E 08	1.718E 09	3.277E 06	8.885E 03
260	1567	1.111E-13	6.334E-04	63.0	22.84	1.457E 09	1.591E 08	1.311E 09	2.967E 06	8.397E 03
280	1615	7.736E-14	4.655E-04	66.9	22.31	9.646E 08	9.977E 07	1.022E 09	2.725E 06	8.037E 03
300	1650	5.525E-14	3.478E-04	70.4	21.79	6.518E 08	6.397E 07	8.093E 08	2.528E 06	7.760E 03
320	1677	4.025E-14	2.635E-04	73.6	21.29	4.470E 08	4.168E 07	6.479E 08	2.363E 06	7.539E 03
340	1696	2.980E-14	2.019E-04	76.7	20.81	3.100E 08	2.749E 07	5.228E 08	2.219E 06	7.357E 03
360	1711	2.237E-14	1.563E-04	79.6	20.36	2.169E 08	1.830E 07	4.246E 08	2.092E 06	7.201E 03
380	1723	1.699E-14	1.221E-04	82.3	19.93	1.528E 08	1.228E 07	3.465E 08	1.978E 06	7.065E 03
400	1732	1.304E-14	9.613E-05	84.9	19.52	1.082E 08	8.289E 06	2.838E 08	1.874E 06	6.944E 03
420	1739	1.010E-14	7.623E-05	87.5	19.15	7.702E 07	5.624E 06	2.333E 08	1.779E 06	6.833E 03
440	1744	7.887E-15	6.084E-05	89.9	18.80	5.504E 07	3.833E 06	1.922E 08	1.690E 06	6.731E 03
460	1748	6.208E-15	4.885E-05	92.2	18.47	3.947E 07	2.623E 06	1.587E 08	1.608E 06	6.635E 03
480	1752	4.920E-15	3.943E-05	94.5	18.18	2.839E 07	1.801E 06	1.314E 08	1.531E 06	6.545E 03
500	1755	3.925E-15	3.198E-05	96.7	17.90	2.048E 07	1.241E 06	1.089E 08	1.459E 06	6.459E 03
520	1757	3.149E-15	2.606E-05	98.7	17.65	1.481E 07	8.572E 05	9.043E 07	1.391E 06	6.376E 03
540	1759	2.540E-15	2.133E-05	100.7	17.42	1.074E 07	5.939E 05	7.521E 07	1.327E 06	6.297E 03
560	1760	2.059E-15	1.752E-05	102.7	17.20	7.806E 06	4.126E 05	6.264E 07	1.267E 06	6.220E 03
580	1761	1.677E-15	1.444E-05	104.5	17.00	5.686E 06	2.873E 05	5.223E 07	1.210E 06	6.145E 03
600	1763	1.372E-15	1.195E-05	106.4	16.82	4.151E 06	2.006E 05	4.362E 07	1.156E 06	6.073E 03
620	1763	1.126E-15	9.917E-06	108.1	16.65	3.036E 06	1.404E 05	3.646E 07	1.104E 06	6.002E 03
640	1764	9.276E-16	8.255E-06	109.9	16.48	2.225E 06	9.845E 04	3.052E 07	1.056E 06	5.933E 03
660	1765	7.667E-16	6.891E-06	111.6	16.33	1.634E 06	6.920E 04	2.558E 07	1.010E 06	5.865E 03
680	1765	6.357E-16	5.768E-06	113.3	16.17	1.202E 06	4.875E 04	2.146E 07	9.659E 05	5.799E 03
700	1766	5.285E-16	4.842E-06	115.1	16.03	8.862E 05	3.441E 04	1.802E 07	9.243E 05	5.735E 03
720	1766	4.406E-16	4.075E-06	116.8	15.88	6.545E 05	2.434E 04	1.515E 07	8.848E 05	5.671E 03
740	1767	3.682E-16	3.438E-06	118.6	15.73	4.842E 05	1.726E 04	1.275E 07	8.471E 05	5.609E 03
760	1767	3.084E-16	2.908E-06	120.5	15.58	3.588E 05	1.226E 04	1.074E 07	8.113E 05	5.548E 03
780	1767	2.590E-16	2.467E-06	122.4	15.43	2.664E 05	8.723E 03	9.057E 06	7.772E 05	5.489E 03
800	1767	2.179E-16	2.097E-06	124.4	15.26	1.981E 05	6.221E 03	7.645E 06	7.448E 05	5.430E 03
820	1768	1.837E-16	1.788E-06	126.5	15.10	1.476E 05	4.445E 03	6.460E 06	7.139E 05	5.372E 03
840	1768	1.552E-16	1.529E-06	128.7	14.92	1.101E 05	3.182E 03	5.464E 06	6.844E 05	5.315E 03
860	1768	1.314E-16	1.311E-06	131.0	14.74	8.233E 04	2.282E 03	4.625E 06	6.564E 05	5.260E 03
880	1768	1.114E-16	1.127E-06	133.6	14.54	6.164E 04	1.640E 03	3.920E 06	6.296E 05	5.205E 03
900	1768	9.469E-17	9.714E-07	136.3	14.33	4.622E 04	1.180E 03	3.325E 06	6.041E 05	5.151E 03
920	1768	8.062E-17	8.401E-07	139.2	14.11	3.472E 04	8.514E 02	2.822E 06	5.797E 05	5.098E 03
940	1768	6.877E-17	7.288E-07	142.3	13.87	2.612E 04	6.151E 02	2.398E 06	5.565E 05	5.046E 03
760	1768	5.877E-17	6.342E-07	145.7	13.62	1.968E 04	4.452E 02	2.040E 06	5.343E 05	4.995E 03
980	1768	5.033E-17	5.538E-07	149.4	13.36	1.485E 04	3.228E 02	1.736E 06	5.131E 05	4.945E 03
1000	1768	4.319E-17	4.853E-07	153.4	13.08	1.123E 04	2.345E 02	1.479E 06	4.929E 05	4.895E 03
1050	1768	3.972E-17	3.542E-07	164.9	12.34	5.612E 03	1.062E 02	9.951E 05	4.462E 05	4.775E 03
1100	1768	2.074E-17	2.647E-07	179.0	11.52	2.832E 03	4.865E 01	6.728E 05	4.044E 05	4.659E 03
1150	1768	1.469E-17	2.026E-07	196.0	10.66	1.442E 03	2.251E 01	4.573E 05	3.670E 05	4.548E 03
1200	1768	1.058E-17	1.589E-07	216.3	9.79	7.407E 02	1.052E 01	3.124E 05	3.335E 05	4.440E 03
1250	1768	7.759E-18	1.276E-07	239.9	8.94	3.839E 02	4.967E 00	2.145E 05	3.035E 05	4.337E 03
1300	1768	5.801E-18	1.047E-07	266.8	8.15	2.007E 02	2.368E 00	1.480E 05	2.765E 05	4.237E 03
1350	1768	4.426E-18	8.762E-08	296.5	7.43	1.058E 02	1.140E 00	1.026E 05	2.522E 05	4.140E 03
1400	1768	3.449E-18	7.464E-08	328.3	6.79	5.622E 01	5.538E-01	7.149E 04	2.303E 05	4.047E 03
1450	1768	2.745E-18	6.456E-08	361.4	6.25	3.012E 01	2.716E-01	5.003E 04	2.106E 05	3.958E 03
1500	1768	2.230E-18	5.656E-08	394.7	5.80	1.627E 01	1.344E-01	3.517E 04	1.927E 05	3.871E 03
1550	1768	1.847E-18	5.008E-08	427.4	5.42	8.855E 00	6.710E 02	2.483E 04	1.766E 05	3.788E 03
1600	1768	1.557E-18	4.473E-08	458.6	5.12	4.857E 00	3.379E-02	1.761E 04	1.620E 05	3.707E 03
1650	1768	1.334E-18	4.025E-08	487.8	4.87	2.684E 00	1.717E-02	1.254E 04	1.488E 05	3.629E 03
1700	1768	1.158E-18	3.643E-08	514.7	4.67	1.494E 00	8.793E 03	8.973E 03	1.368E 05	3.553E 03
1750	1768	1.018E-18	3.313E-08	539.3	4.52	8.376E-01	4.542E-03	6.444E 03	1.258E 05	3.480E 03
1800	1768	9.037E-19	3.026E-08	561.6	4.39	4.730E-01	2.365E-03	4.647E 03	1.159E 05	3.409E 03
1850	1768	8.092E-19	2.772E-08	581.7	4.29	2.689E-01	1.241E-03	3.365E 03	1.069E 05	3.341E 03
1900	1768	7.296E-19	2.547E-08	600.0	4.21	1.540E-01	6.564E-04	2.446E 03	9.867E 04	3.275E 03
1950	1768	6.618E-19	2.346E-08	616.8	4.15	8.874E-02	3.449E-04	1.784E 03	9.116E 04	3.210E 03
2000	1768	6.032E-19	2.166E-08	632.2	4.09	5.149E-02	1.879E-04	1.307E 03	8.430E 04	3.148E 03
2050	1768	5.520E-19	2.003E-08	646.5	4.05	3.006E-02	1.016E-04	9.607E 02	7.803E 04	3.088E 03

TABLE 5. Properties of the upper atmosphere for 18,000^b local time as a function of altitude from 120 to 2050 km
 $(\cos\theta = -1.2703 \times 10^{-6}$ Int grad = 1.6811E 01).

Alt km	Temp K	Density gm cm ⁻³	Pressure dyne cm ⁻²	Scale ht km	Mean mol wt	N(N ₂) cm ⁻³	N(O ₂) cm ⁻³	N(O) cm ⁻³	N(He) cm ⁻³	N(H) cm ⁻³
120	355	3.536E-11	3.802E-02	11.4	27.46	5.800E 11	1.200E 11	7.600E 10	2.500E 07	4.356E 04
130	514	1.172E-11	1.856E-02	16.8	26.98	1.916E 11	3.570E 10	3.443E 10	1.553E 07	2.930E 04
140	658	5.366E-12	1.105E-02	21.9	26.56	8.698E 10	1.501E 10	1.971E 10	1.122E 07	2.244E 04
150	787	2.929E-12	7.322E-03	26.7	26.18	4.695E 10	7.612E 09	1.283E 10	8.809E 06	1.847E 04
160	900	1.787E-12	5.178E-03	31.1	25.82	2.827E 10	4.348E 09	9.066E 09	7.303E 06	1.594E 04
170	997	1.176E-12	3.825E-03	35.0	25.47	1.833E 10	2.690E 09	6.773E 09	6.287E 06	1.422E 04
180	1080	8.159E-13	2.913E-03	38.5	25.14	1.252E 10	1.761E 09	5.263E 09	5.559E 06	1.299E 04
190	1150	5.890E-13	2.270E-03	41.7	24.81	8.888E 09	1.201E 09	4.210E 09	5.013E 06	1.207E 04
200	1210	4.382E-13	1.800E-03	44.6	24.49	6.490E 09	8.446E 08	3.441E 09	4.587E 06	1.136E 04
220	1305	2.589E-13	1.178E-03	49.6	23.86	3.680E 09	4.466E 08	2.408E 09	3.963E 06	1.035E 04
240	1375	1.628E-13	8.009E-04	54.0	23.24	2.207E 09	2.510E 08	1.758E 09	3.521E 06	9.664E 03
260	1427	1.069E-13	5.603E-04	57.9	22.63	1.375E 09	1.469E 08	1.320E 09	3.187E 06	9.167E 03
280	1466	7.247E-14	4.008E-04	61.5	22.04	8.791E 08	8.853E 07	1.010E 09	2.920E 06	8.789E 03
300	1496	5.041E-14	2.920E-04	64.8	21.48	5.730E 08	5.446E 07	7.841E 08	2.700E 06	8.490E 03
320	1518	3.580E-14	2.159E-04	67.8	20.93	3.789E 08	3.403E 07	6.149E 08	2.511E 06	8.245E 03
340	1536	2.587E-14	1.618E-04	70.8	20.42	2.534E 08	2.153E 07	4.861E 08	2.347E 06	8.038E 03
360	1549	1.898E-14	1.226E-04	73.5	19.94	1.709E 08	1.375E 07	3.866E 08	2.202E 06	7.859E 03
380	1560	1.411E-14	9.388E-05	76.2	19.49	1.161E 08	8.853E 06	3.091E 08	2.071E 06	7.700E 03
400	1568	1.061E-14	7.253E-05	78.8	19.07	7.939E 07	5.737E 06	2.481E 08	1.952E 06	7.557E 03
420	1575	8.061E-15	5.648E-05	81.2	18.69	5.455E 07	3.740E 06	1.998E 08	1.843E 06	7.426E 03
440	1580	6.184E-15	4.430E-05	83.5	18.34	3.764E 07	2.449E 06	1.613E 08	1.742E 06	7.304E 03
460	1584	4.784E-15	3.497E-05	85.7	18.02	2.608E 07	1.611E 06	1.306E 08	1.649E 06	7.190E 03
480	1588	3.730E-15	2.777E-05	87.8	17.73	1.813E 07	1.064E 06	1.060E 08	1.562E 06	7.082E 03
500	1590	2.928E-15	2.217E-05	89.8	17.46	1.264E 07	7.053E 05	8.619E 07	1.481E 06	6.979E 03
520	1593	2.313E-15	1.779E-05	91.8	17.22	8.843E 06	4.690E 05	7.021E 07	1.405E 06	6.880E 03
540	1595	1.838E-15	1.434E-05	93.6	17.00	6.203E 06	3.129E 05	5.729E 07	1.334E 06	6.785E 03
560	1596	1.468E-15	1.160E-05	95.4	16.79	4.362E 06	2.094E 05	4.682E 07	1.267E 06	6.693E 03
580	1598	1.178E-15	9.425E-06	97.1	16.60	3.076E 06	1.405E 05	3.832E 07	1.204E 06	6.604E 03
600	1599	9.493E-16	7.685E-06	98.8	16.42	2.174E 06	9.453E 04	3.141E 07	1.145E 06	6.518E 03
620	1600	7.681E-16	6.288E-06	100.5	16.25	1.540E 06	6.377E 04	2.578E 07	1.089E 06	6.434E 03
640	1601	6.237E-16	5.162E-06	102.2	16.08	1.093E 06	4.313E 04	2.119E 07	1.036E 06	6.352E 03
660	1601	5.082E-16	4.251E-06	103.9	15.91	7.779E 05	2.924E 04	1.744E 07	9.863E 05	6.272E 03
680	1602	4.153E-16	3.513E-06	105.6	15.75	5.547E 05	1.988E 04	1.437E 07	9.392E 05	6.194E 03
700	1603	3.404E-16	2.911E-06	107.4	15.58	3.964E 05	1.354E 04	1.185E 07	8.947E 05	6.117E 03
720	1603	2.798E-16	2.421E-06	109.3	15.41	2.838E 05	9.248E 03	9.790E 06	8.525E 05	6.042E 03
740	1604	2.306E-16	2.019E-06	111.2	15.23	2.036E 05	6.330E 03	8.095E 06	8.126E 05	5.969E 03
760	1604	1.905E-16	1.690E-06	113.3	15.04	1.464E 05	4.342E 03	6.702E 06	7.749E 05	5.898E 03
780	1604	1.578E-16	1.419E-06	115.5	14.83	1.054E 05	2.985E 03	5.555E 06	7.391E 05	5.828E 03
800	1605	1.310E-16	1.195E-06	117.9	14.62	7.609E 04	2.057E 03	4.609E 06	7.051E 05	5.759E 03
820	1605	1.090E-16	1.011E-06	120.5	14.39	5.501E 04	1.420E 03	3.828E 06	6.730E 05	5.691E 03
840	1605	9.088E-17	8.576E-07	123.3	14.14	3.985E 04	9.829E 02	3.183E 06	6.424E 05	5.625E 03
860	1605	7.597E-17	7.306E-07	126.3	13.88	2.892E 04	6.816E 02	2.650E 06	6.135E 05	5.560E 03
880	1605	6.366E-17	6.249E-07	129.7	13.60	2.103E 04	4.736E 02	2.208E 06	5.860E 05	5.496E 03
900	1605	5.347E-17	5.367E-07	133.3	13.30	1.531E 04	3.298E 02	1.842E 06	5.598E 05	5.434E 03
920	1605	4.502E-17	4.630E-07	137.3	12.98	1.117E 04	2.301E 02	1.538E 06	5.350E 05	5.372E 03
940	1606	3.800E-17	4.011E-07	141.7	12.65	8.167E 03	1.609E 02	1.285E 06	5.115E 05	5.312E 03
960	1606	3.216E-17	3.491E-07	146.6	12.30	5.979E 03	1.127E 02	1.075E 06	4.890E 05	5.253E 03
980	1606	2.730E-17	3.053E-07	151.8	11.93	4.385E 03	7.908E 01	9.006E 05	4.677E 05	5.195E 03
1000	1606	2.323E-17	2.683E-07	157.6	11.56	3.222E 03	5.561E 01	7.550E 05	4.475E 05	5.137E 03
1050	1606	1.573E-17	1.984E-07	174.4	10.59	1.501E 03	2.325E 01	4.878E 05	4.010E 05	4.998E 03
1100	1606	1.088E-17	1.512E-07	194.9	9.60	7.069E 02	9.838E 00	3.170E 05	3.599E 05	4.865E 03
1150	1606	7.696E-18	1.187E-07	219.2	8.66	3.361E 02	4.210E 00	2.072E 05	3.234E 05	4.737E 03
1200	1606	5.583E-18	9.573E-08	246.9	7.78	1.614E 02	1.822E 00	1.362E 05	2.911E 05	4.614E 03
1250	1606	4.158E-18	7.908E-08	277.5	7.02	7.827E 01	7.970E-01	9.002E 04	2.623E 05	4.495E 03
1300	1606	3.182E-18	6.669E-08	309.9	6.37	3.831E 01	3.525E-01	5.982E 04	2.367E 05	4.381E 03
1350	1606	2.500E-18	5.720E-08	342.7	5.83	1.893E 01	1.576E-01	3.996E 04	2.139E 05	4.272E 03
1400	1606	2.014E-18	4.976E-08	374.8	5.40	9.435E 00	7.116E-02	2.684E 04	1.936E 05	4.166E 03
1450	1606	1.660E-18	4.377E-08	405.1	5.06	4.746E 00	3.246E-02	1.811E 04	1.754E 05	4.065E 03
1500	1606	1.396E-18	3.885E-08	433.1	4.80	2.408E 00	1.496E-02	1.229E 04	1.591E 05	3.967E 03
1550	1606	1.194E-18	3.473E-08	458.3	4.59	1.232E 00	6.961E-03	8.376E 03	1.445E 05	3.873E 03
1600	1606	1.037E-18	3.122E-08	480.8	4.43	6.359E-01	3.271E-03	5.737E 03	1.314E 05	3.782E 03
1650	1606	9.103E-19	2.820E-08	500.7	4.31	3.309E-01	1.551E-03	3.948E 03	1.196E 05	3.694E 03
1700	1606	8.070E-19	2.556E-08	518.4	4.21	1.736E-01	7.425E-04	2.730E 03	1.090E 05	3.609E 03
1750	1606	7.209E-19	2.325E-08	534.3	4.14	9.178E-02	3.586E-04	1.896E 03	9.949E 04	3.528E 03
1800	1606	6.481E-19	2.120E-08	548.6	4.08	4.891E-02	1.748E-04	1.323E 03	9.089E 04	3.449E 03
1850	1606	5.856E-19	1.937E-08	561.7	4.04	2.626E-02	8.593E-05	9.267E 02	8.313E 04	3.373E 03
1900	1606	5.312E-19	1.774E-08	573.9	4.00	1.421E-02	4.261E-05	6.522E 02	7.611E 04	3.299E 03
1950	1606	4.836E-19	1.627E-08	585.3	3.97	7.745E-03	2.131E-05	4.609E 02	6.975E 04	3.228E 03
2000	1606	4.415E-19	1.495E-08	596.3	3.94	4.252E-03	1.074E-05	3.271E 02	6.399E 04	3.159E 03
2050	1606	4.040E-19	1.376E-08	606.8	3.92	2.351E-03	5.462E-06	2.330E 02	5.877E 04	3.093E 03

TABLE 6. Properties of the upper atmosphere for 22,000^b local time as a function of altitude from 120 to 2050 km
(cosθ = 8.6602E-01 Int grad = 1.7229E 01).

Alt km	Temp K	Density gm cm ⁻³	Pressure dyne cm ⁻²	Scale ht km	Mean mol wt	N(N ₂) cm ⁻³	N(O ₂) cm ⁻³	N(O) cm ⁻³	N(He) cm ⁻³	N(H) cm ⁻³
120	355	3.536E-11	3.802E-02	11.4	27.46	5.800E 11	1.200E 11	7.600E 10	2.500E 07	4.356E 04
130	515	1.172E-11	1.860E-02	16.9	26.98	1.916E 11	3.571E 10	3.439E 10	1.550E 07	2.924E 04
140	651	5.424E-12	1.106E-02	21.7	26.56	8.792E 10	1.517E 10	1.992E 10	1.134E 07	2.268E 04
150	765	2.991E-12	7.265E-03	26.0	26.17	4.793E 10	7.762E 09	1.315E 10	9.057E 06	1.901E 04
160	858	1.834E-12	5.070E-03	29.6	25.80	2.900E 10	4.444E 09	9.389E 09	7.638E 06	1.671E 04
170	933	1.206E-12	3.680E-03	32.8	25.43	1.877E 10	2.738E 09	7.062E 09	6.676E 06	1.517E 04
180	994	8.330E-13	2.747E-03	35.6	25.06	1.274E 10	1.774E 09	5.505E 09	5.981E 06	1.407E 04
190	1043	5.959E-13	2.093E-03	38.0	24.70	8.934E 09	1.191E 09	4.402E 09	5.453E 06	1.326E 04
200	1083	4.377E-13	1.620E-03	40.2	24.34	6.423E 09	8.217E 08	3.587E 09	5.035E 06	1.264E 04
220	1143	2.503E-13	1.007E-03	43.9	23.61	3.495E 09	4.131E 08	2.475E 09	4.409E 06	1.175E 04
240	1182	1.512E-13	6.492E-04	47.2	22.88	1.990E 09	2.182E 08	1.768E 09	3.949E 06	1.114E 04
260	1209	9.492E-14	4.303E-04	50.1	22.17	1.167E 09	1.190E 08	1.290E 09	3.589E 06	1.070E 04
280	1227	6.139E-14	2.917E-04	52.8	21.47	6.977E 08	6.629E 07	9.552E 08	3.290E 06	1.035E 04
300	1240	4.068E-14	2.015E-04	55.4	20.81	4.230E 08	3.749E 07	7.143E 08	3.035E 06	1.007E 04
320	1249	2.752E-14	1.415E-04	57.9	20.18	2.591E 08	2.145E 07	5.380E 08	2.811E 06	9.821E 03
340	1255	1.895E-14	1.009E-04	60.2	19.61	1.600E 08	1.237E 07	4.074E 08	2.612E 06	9.605E 03
360	1260	1.326E-14	7.282E-05	62.5	19.08	9.941E 07	7.190E 06	3.098E 08	2.432E 06	9.408E 03
380	1263	9.414E-15	5.317E-05	64.7	18.60	6.209E 07	4.203E 06	2.364E 08	2.267E 06	9.227E 03
400	1266	6.770E-15	3.921E-05	66.7	18.17	3.896E 07	2.469E 06	1.809E 08	2.117E 06	9.056E 03
420	1268	4.925E-15	2.918E-05	68.7	17.79	2.455E 07	1.457E 06	1.388E 08	1.978E 06	8.894E 03
440	1269	3.619E-15	2.189E-05	70.5	17.45	1.552E 07	8.634E 05	1.067E 08	1.850E 06	8.739E 03
460	1270	2.685E-15	1.654E-05	72.2	17.14	9.848E 06	5.136E 05	8.225E 07	1.732E 06	8.589E 03
480	1271	2.008E-15	1.258E-05	73.9	16.87	6.268E 06	3.067E 05	6.350E 07	1.622E 06	8.445E 03
500	1272	1.512E-15	9.625E-06	75.5	16.62	4.002E 06	1.837E 05	4.911E 07	1.520E 06	8.305E 03
520	1273	1.147E-15	7.404E-06	77.0	16.39	2.563E 06	1.104E 05	3.805E 07	1.425E 06	8.170E 03
540	1273	8.745E-16	5.726E-06	78.6	16.17	1.646E 06	6.661E 04	2.953E 07	1.337E 06	8.037E 03
560	1274	6.704E-16	4.450E-06	80.1	15.95	1.060E 06	4.030E 04	2.295E 07	1.255E 06	7.909E 03
580	1274	5.164E-16	3.475E-06	81.7	15.74	6.843E 05	2.446E 04	1.787E 07	1.178E 06	7.783E 03
600	1274	3.995E-16	2.727E-06	83.3	15.52	4.431E 05	1.489E 04	1.393E 07	1.106E 06	7.661E 03
620	1275	3.103E-16	2.151E-06	85.1	15.29	2.876E 05	9.089E 03	1.088E 07	1.039E 06	7.541E 03
640	1275	2.419E-16	1.705E-06	87.0	15.04	1.872E 05	5.566E 03	8.511E 06	9.771E 05	7.424E 03
660	1275	1.893E-16	1.358E-06	89.1	14.78	1.221E 05	3.418E 03	6.666E 06	9.188E 05	7.310E 03
680	1275	1.487E-16	1.088E-06	91.4	14.49	7.990E 04	2.105E 03	5.229E 06	8.644E 05	7.198E 03
700	1276	1.172E-16	8.769E-07	94.0	14.18	5.240E 04	1.300E 03	4.107E 06	8.134E 05	7.088E 03
720	1276	9.271E-17	7.111E-07	96.9	13.83	3.445E 04	8.055E 02	3.231E 06	7.658E 05	6.982E 03
740	1276	7.361E-17	5.804E-07	100.2	13.45	2.270E 04	5.003E 02	2.545E 06	7.211E 05	6.877E 03
760	1276	5.866E-17	4.771E-07	103.9	13.05	1.499E 04	3.116E 02	2.007E 06	6.794E 05	6.775E 03
780	1276	4.694E-17	3.950E-07	108.1	12.61	9.929E 03	1.946E 02	1.586E 06	6.403E 05	6.674E 03
800	1276	3.772E-17	3.296E-07	112.9	12.14	6.590E 03	1.219E 02	1.254E 06	6.036E 05	6.576E 03
820	1276	3.044E-17	2.772E-07	118.3	11.66	4.384E 03	7.651E 01	9.933E 05	5.692E 05	6.480E 03
840	1277	2.469E-17	2.350E-07	124.4	11.15	2.923E 03	4.817E 01	7.877E 05	5.370E 05	6.386E 03
860	1277	2.013E-17	2.009E-07	131.1	10.63	1.953E 03	3.040E 01	6.255E 05	5.068E 05	6.294E 03
880	1277	1.650E-17	1.732E-07	138.7	10.11	1.308E 03	1.924E 01	4.973E 05	4.784E 05	6.204E 03
900	1277	1.360E-17	1.506E-07	147.1	9.59	8.783E 02	1.220E 01	3.959E 05	4.518E 05	6.116E 03
920	1277	1.128E-17	1.320E-07	156.2	9.08	5.909E 02	7.761E 00	3.156E 05	4.268E 05	6.029E 03
940	1277	9.423E-18	1.166E-07	166.1	8.58	3.984E 02	4.948E 00	2.519E 05	4.033E 05	5.944E 03
960	1277	7.923E-18	1.037E-07	176.7	8.11	2.692E 02	3.162E 00	2.013E 05	3.812E 05	5.861E 03
980	1277	6.710E-18	9.293E-08	188.0	7.66	1.823E 02	2.026E 00	1.611E 05	3.604E 05	5.779E 03
1000	1277	5.724E-18	8.382E-08	199.9	7.25	1.237E 02	1.301E 00	1.290E 05	3.409E 05	5.699E 03
1050	1277	3.977E-18	6.643E-08	231.1	6.36	4.736E 01	4.347E-01	7.450E 04	2.970E 05	5.506E 03
1100	1277	2.894E-18	5.424E-08	262.9	5.66	1.837E 01	1.474E-01	4.333E 04	2.592E 05	5.322E 03
1150	1277	2.198E-18	4.531E-08	293.0	5.15	7.212E 00	5.068E-02	2.539E 04	2.266E 05	5.146E 03
1200	1277	1.733E-18	3.849E-08	319.9	4.78	2.868E 00	1.768E-02	1.498E 04	1.985E 05	4.979E 03
1250	1277	1.408E-18	3.310E-08	343.0	4.52	1.154E 00	6.252E-03	8.898E 03	1.742E 05	4.818E 03
1300	1277	1.172E-18	2.873E-08	362.5	4.33	4.699E-01	2.241E-03	5.322E 03	1.531E 05	4.666E 03
1350	1277	9.930E-19	2.511E-08	378.7	4.20	1.936E-01	8.141E-04	3.205E 03	1.348E 05	4.519E 03
1400	1277	8.528E-19	2.205E-08	392.3	4.11	8.068E-02	2.996E-04	1.942E 03	1.188E 05	4.379E 03
1450	1277	7.398E-19	1.945E-08	404.1	4.04	3.400E-02	1.117E-04	1.185E 03	1.050E 05	4.246E 03
1500	1277	6.465E-19	1.722E-08	414.5	3.99	1.449E-02	4.216E-05	7.273E 02	9.286E 04	4.117E 03
1550	1277	5.682E-19	1.528E-08	423.9	3.95	6.238E-03	1.611E-05	4.492E 02	8.227E 04	3.995E 03
1600	1277	5.016E-19	1.360E-08	432.7	3.92	2.715E-03	6.232E-06	2.791E 02	7.301E 04	3.877E 03
1650	1277	4.443E-19	1.213E-08	441.1	3.89	1.194E-03	2.439E-06	1.745E 02	6.488E 04	3.764E 03
1700	1277	3.947E-19	1.084E-08	449.3	3.87	5.306E-04	9.657E-07	1.097E 02	5.774E 04	3.656E 03
1750	1277	3.516E-19	9.706E-09	457.5	3.85	2.381E-04	3.868E-07	6.935E 01	5.146E 04	3.553E 03
1800	1277	3.138E-19	8.710E-09	465.6	3.82	1.079E-04	1.567E-07	4.410E 01	4.593E 04	3.453E 03
1850	1277	2.806E-19	7.830E-09	473.8	3.80	4.937E-05	6.415E-08	2.820E 01	4.105E 04	3.357E 03
1900	1277	2.514E-19	7.053E-09	482.2	3.78	2.280E-05	2.655E-08	1.813E 01	3.674E 04	3.266E 03
1950	1277	2.256E-19	6.364E-09	490.8	3.76	1.063E-05	1.111E-08	1.171E 01	3.293E 04	3.177E 03
2000	1277	2.027E-19	5.752E-09	499.5	3.74	5.002E-06	4.696E-09	7.610E 00	2.955E 04	3.092E 03
2050	1277	1.825E-19	5.209E-09	508.5	3.72	2.374E-06	2.005E-09	4.969E 00	2.655E 04	3.011E 03